

M

Report No. 66.69E

Second Quarterly Report For

AN ADVANCED BRUSHLESS DC TORQUE MOTOR

30 September 1966 - 30 December 1966

Contract No. NAS 5-10263

Prepared By

WESTINGHOUSE ELECTRIC CORPORATION
AEROSPACE ELECTRICAL DIVISION
LIMA, OHIO

For

GODDARD SPACE FLIGHT CENTER
GREENBELT, MARYLAND

N 68-14644

FACILITY FORM 602

(ACCESSION NUMBER)	(THRU)
<i>79</i>	<i>1</i>
(PAGES)	(CODE)
<i>CR-91686</i>	<i>09</i>
(NASA CR OR TMX OR AD NUMBER)	(CATEGORY)

GPO PRIC	\$	
CFSTI PRIC	\$	
Hard cc	(C)	<i>B-02</i>
Microfrc	(F)	<i>165</i>

ff 653 July 65

297-48866

Second Quarterly Report For
AN ADVANCED BRUSHLESS DC TORQUE MOTOR
30 September 1966 - 30 December 1966

Contract No. NAS 5-10263

Prepared By

WESTINGHOUSE ELECTRIC CORPORATION
AEROSPACE ELECTRICAL DIVISION
LIMA, OHIO


For

GODDARD SPACE FLIGHT CENTER
GREENBELT, MARYLAND


Prepared by:



W. W. Yates
Equipment Systems Section




D. E. Baker
Standard Apparatus Section

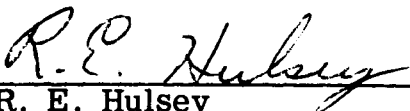


R. E. Skamfer
Standard Apparatus Section


Approved by:



W. E. Wier
Mgr. Equipment Systems Section



R. E. Hulsey
Mgr. Standard Apparatus Section



F. J. Bertoldo
Sales Manager, USD Marketing

ABSTRACT

This report covers the work performed on NASA contract NAS 5-10263 during the second quarter of work commencing September 30, 1966 and ending December 30, 1966. This contract covers the development of an advanced version of a brushless d-c torque motor using magnetic sensing of position. The motor will combine the functions of speed control and commutation, and in addition will provide position and rate information.

During the above period, the final detailed design of the motor-controller was completed. Drawings were completed and critical items advance ordered. A final breadboard of the control circuit was completed and operated successfully. No problems are foreseen in making a successful unit.

LIST OF FIGURES

FIGURE	TITLE	PAGE
1	Motor Armature Punching	8
2	Permanent Magnet Rotor	9
3	Magnetic Sensor Rotor Core	12
4	Magnetic Sensor Stator Core	13
5	Magnetic Sensor Winding Diagram	14
6	Equivalent Half-Circuit for Magnetic Sensor	17
7	Fully Linked Output Voltage Pulse Versus Time	22
8	Switching Characteristics with Inductive Load - PNP Transistor 2N3201	23
9	Controller-Commutator Circuit Schematic	24
10	Mechanical Configuration	27
11	Motor-Controller Outline	32
12	Pulse Width Versus Signal Voltage	34
13	Calculated Speed-Torque Curves Versus Speed-Control Signal Voltage	35
14	Detail of Amplitude Envelope Pulse	37
15	Amplitude of Sensor Output Signals Versus Angular Position.	38

Note: Figures used in APPENDIX I are not included.

LIST OF TABLES

TABLE	TITLE	PAGE
1	Dimensions	3
2	Motor Design Characteristics	10
3	Magnetic Sensor Design Characteristics	18
4	Magnetic Sensor Half-Circuit Constants	19
5	Solid State Component Derating Practice	25
6	Material List	31

Note: Tables used in APPENDIX I are not included.

SECTION I
INTRODUCTION

A. PURPOSE

The purpose of the effort on this contract is to develop an advanced version of a brushless d-c torque motor and controller. A previous version was built on NASA contract NAS 5-3934. The new motor-controller will use a simple magnetic sensor which will sense position for commutation and also provide position and rate information for control purposes. Other advanced features, in addition to the commutator function, will include speed control with pulse-width-modulation using a variable input control voltage, reverseability using only one sensor in response to input signal voltages, stand-by operation with zero power draw in response to an input signal, lower ripple torque than the previous version, insensitivity to line voltage variation, use of only one constant voltage supply, and miniaturization of the control circuit. The motor is designed specifically for use in orientation systems for solar arrays on space vehicles.

Other specification requirements of the motor are listed below:

- 1) The circuit will be designed for maximum simplicity and reliability with a design goal of less than 100 components.
- 2) Maximum angular resolution consistent with other performance factors will be obtained.
- 3) The motor and control will be as small and as lightweight as possible.
- 4) The motor will provide a minimum of 90 ounce-inches of torque at stall, with 28 volts applied. Maximum average current under these conditions will be 0.4 amps.
- 5) The motor will be provided with a 1.5 inch diameter hollow shaft and will have a maximum OD of 4.00 inches. The total package weight will be approximately 4.5 pounds.

- 6) Peak-to-peak ripple torque will be a maximum of 15 percent of the average torque or 0.5 ounce-inches, whichever is larger.
- 7) The magnetic rotor position sensor will be designed to operate at 10 kc/s.
- 8) The motor will be capable of continuous operation at speeds up to 100 rpm.
- 9) The motor will be designed to operate in a vacuum of 1×10^{-9} mm hg for 5 years.
- 10) The motor will operate properly over an ambient temperature range of -10°C to $+70^{\circ}\text{C}$.
- 11) The motor will operate properly after 50 g, 2 msec shock and 5 minutes of random vibration from 20 to 2000 c/s at 15 g rms in each of three mutually perpendicular directions.

This report covers the second quarter of work which includes the detailed design and drafting. Previous work determined the feasibility of the methods used.

B. SUMMARY OF WORK PERFORMED

A detailed design of the motor-controller was made in this quarter. Complete manufacturing drawings were also made. Critical delivery parts were advance ordered.

A breadboard of the controller-commutator circuit was made of the final detail design using actual parts to be used in the final motor-controller. Operational tests were made to determine proper functioning of all parts of the circuit.

The electrical design is broken up into three major areas: the motor, magnetic sensor, and controller-commutator circuit. The mechanical design is composed of two major areas; the motor and sensor package, and the circuit package. The two packages can be operated separately or combined.

TABLE OF CONTENTS

SECTION	PAGE
LIST OF FIGURES	v
LIST OF TABLES	vi
I INTRODUCTION	1
A. Purpose	1
B. Summary of Work Performed	2
II DISCUSSION	3
A. Dimensions	3
B. Motor Electrical Design	3
1. General Description	3
2. Design Criteria and Assumptions	4
3. Design	6
4. Time Constant	7
C. Magnetic Sensor Design	11
1. General Description	11
2. Core Design	11
3. Winding Design	15
D. Controller-Commutator Circuit Design	21
1. General Description	21
2. Circuit Changes	21
3. Design	25
E. Mechanical Design	26
1. General Discussion	26
2. Manufacturing Procedure	26
3. Specific Comments	28
a. Bearing System	28
b. Structural Integrity of Sensor Cores	29
4. Weight Estimate	29
5. Materials and Finishes	30
F. Operating Characteristics	30
1. Physical Configuration	30
2. Forward, Reverse, and Standby	30
3. Speed Control	30

TABLE OF CONTENTS (Cont.)

SECTION	PAGE
4. Rate and Position Information	36
G. Testing Procedure	39
1. Design of Magnetic Sensor	39
2. Engineering Tests	39
3. Laboratory Tests	40
III NEW TECHNOLOGY	44
IV PROGRAM FOR NEXT REPORTING INTERVAL	45
V CONCLUSIONS AND RECOMMENDATIONS	46
VI BIBLIOGRAPHY	47
VII APPENDIX I - Controller-Commutator Circuit Description - Previous Version	48

SECTION II

DISCUSSION

A. DIMENSIONS

In this discussion the following dimensions are used throughout.

Length - inches
Weight - pounds
Area - square inches
Volume - cubic inches
Torque - ounce-inches
Magnetic Flux - lines or Maxwells
Magnetic Density - lines per square inch
Magnetic Field Intensity - ampere-turns per inch.
Magnetomotive Force (mmf) - ampere-turns
Permeance - Maxwells per ampere-turn
Temperature - degrees centigrade
Voltage - volts
Current - amperes
Power - watts
Resistance - ohms
Capacitance - microfarads
Inductance - henries

TABLE 1. DIMENSIONS

B. MOTOR ELECTRICAL DESIGN

1. General Description

The work in the previous quarter determined that the motor should be a permanent magnet type to obtain the greatest torque to weight ratio and the least ripple torque. The permanent magnet will be contained on the rotor; the armature will be stationary. The optimum configuration was determined to be a 16 pole motor with a 3-circuit armature connected in delta.

2. Design Criteria and Assumptions

Fixed Inputs

- (a) Armature punching OD = 3.812 - obtained from the limiting motor OD and frame thickness.
- (b) Magnet ID = 1.563 - obtained from the shaft OD and bearing bore.
- (c) Torque Output = 90 ounce-inches minimum at 0.4 amps average maximum with 28 volts applied. The average voltage that the motor sees with halfwave modulation is 14 volts minus the forward transistor drop. The current thus drawn is 0.8 amps at 14 volts.
- (d) Ripple Torque = 15 percent maximum.
- (e) Forward transistor voltage drop = 1.2 volts.

Initial Design Decisions - The following characteristic values have been determined from past experience as being satisfactory, close-to-optimum, or practical.

- (a) Pole enclosure - 0.667
- (b) Stator punching slot opening - 0.05
- (c) Stator punching tooth tip thickness - 0.025.
- (d) Thickness allowed for slot insulation - 0.008
- (e) Stator punching stacking factor - 0.95.
- (f) Bore can thickness - it has been found necessary to use a thin magnetic tube in the stator bore to decrease cogging. This can will be made of a 0.006 inch thick 50 percent nickel steel (Westinghouse Hipernik).

Materials

- (a) Permanent Magnet - Alnico V. The magnet rotor will be a one-piece casting. Although higher energy magnets are available, these cannot be magnetized in a one piece casting since they can only be magnetized in a straight line. To use them would

require a fabricated rotor. With the short stack length of this motor, it would cost approximately as much weight to fabricate the rotor as it does to provide additional stack length to make up the difference in magnet energy and would be more costly and complicated.

- (b) Armature Insulation - The insulation system will be composed mostly of products related to the polyimide type of insulation. DuPont ML enamelled wire and Pyre ML (glass and ML resin) slot liners and Westinghouse Doryl varnish will be used. Silicone glass wedges and some teflon lacing cord will also be used. Leads will have teflon insulation. This system has high temperature capabilities and low vacuum outgassing characteristics.
- (c) Westinghouse Electrical Steel - Hiperco 50. This steel is among the best in having the highest flux density capability and the highest permeability at high densities. A lamination thickness of 0.010 inch will be used. Punchings will be insulated with a coating of aluminum orthophosphate to minimize high frequency core loss.

Heat Factor

Since the mounting of the motor in the application is unknown, it is not possible to determine the actual operating temperature of the motor in a vacuum. The previous motor had a temperature rise in room ambient temperature and pressure of 65°C with 36.6 watts loss with no conductive cooling. Since this motor will have approximately 10.3 watts loss at full speed locked rotor and is larger, a temperature rise of approximately 15°C is expected under the same conditions. This will tend to be higher in a vacuum, but the addition of conductive cooling will decrease it. Also, ambient temperature is quite variable. In view of the unpredictability of actual operating conditions, the specification limits were assumed to apply at a winding temperature of 40°C which is the expected temperature rise under room conditions. Higher temperatures will decrease the torque and lower current; lower temperature will do the opposite.

3. Design

Number of Stator Punching Slots and Ripple Torque

The first step in the design is the determination of the number of stator slots. Since at least one slot per armature circuit per pole is needed, there must be at least 48 slots. However, to reduce cogging, it is necessary to minimize the permeance variation between the rotor magnet and the stator at the air gap as the magnet rotates. This can be done by making the number of stator slots not evenly divisible by the number of poles. It is also desired to keep the number of slots to a minimum to keep the stator teeth from becoming too thin mechanically. The lowest number of slots which accomplishes the above and still allows a balanced three-circuit winding is 51. Therefore, 51 slots were selected. The theoretically zero variance in permeance plus the magnetic can in the bore should make cogging torque a minimum.

The next consideration is that of ripple torque. If slot openings are disregarded and a sinusoidal space distribution of air gap magnetic flux density is assumed with one slot per armature circuit per pole, the ripple torque can be calculated as exceeding 14 percent. If a quasi-square wave of density is assumed and slot openings are disregarded, the theoretical ripple torque is zero. However, slot openings cannot be disregarded and therefore a layout of slots is necessary to obtain a value for ripple torque. Such a layout was made of the 51 slot stator with the 16 pole rotor assuming a quasi-square flux density wave. Zero skew was used with a coil throw of 3 slots. The rotor was moved under the slots to the theoretical extremes and middle of the switching angle. Conductors in the field were counted and together with the current in the conductors, this figure was used to calculate the ripple torque. The actual figure obtained was 1.09 percent ripple. It is felt that the ripple will exceed this because of irregularities in the manufacture, the deviation of the flux density wave from the quasi-square ideal, and departure from the ideal switching points, but the figure does indicate that the ripple will be small. Skewing could be utilized to lower cogging torque slightly, but this would entail some sacrifice in ripple torque and average torque.

Stator and Rotor Magnetic Design

The object of the design is to use the magnetic materials to the fullest with some margin for conservatism to be reliable. That is, the operating point on the magnet should be such as to obtain the maximum flux with sufficient mmf reserve to avoid demagnetization and the magnetic steel in the stator should be worked at its highest capabilities. When the above is done, the highest torque per pound of weight with the required input power limitation should be obtained.

The same design methods described in the final report on NASA contract NAS5-3934, "Final Report for a Brushless DC Torque Motor", Report No. CR-374, dated February, 1966, were used. Considerable iteration is necessary to determine the final design. It was necessary to increase the thickness of the section between the stator OD and the slots slightly above the magnetic optimum for mechanical reasons. Also it was found in the final design that the mmf capability of the magnet was used very conservatively, primarily due to the necessity for making the slot area fit an integral wire size. That is, the magnet OD could have been lowered from an mmf standpoint, but not enough to increase the slot area sufficiently to allow use of the next wire size. Therefore, the design would suffer since there would effectively be no increase in wire size and flux would be lowered. Consequently, the excess mmf capability was used to increase the air gap length from 0.008 to 0.010 which will help to lower cogging torque.

The final design of the stator punching is shown in Figure 1. The final design of the rotor magnet is shown in Figure 2. Complete calculated design characteristics are given in Table 2.

4. Time Constant

Tests on the previous unit, which were reported in the previous quarterly report, indicated the time constant of the previous motor was approximately 0.002 seconds. Calculations were made which approximately agreed with the tested value. The same calculation procedures were used to determine the time constant of this design. The results gave a calculated value of 0.0018 seconds. Therefore, the two designs will have approximately the same time constant. This was shown to be acceptable in the tests on the previous motor; that is, there was no appreciable variation in motor current when a half-wave pulsed 10 kc/sec voltage was applied.

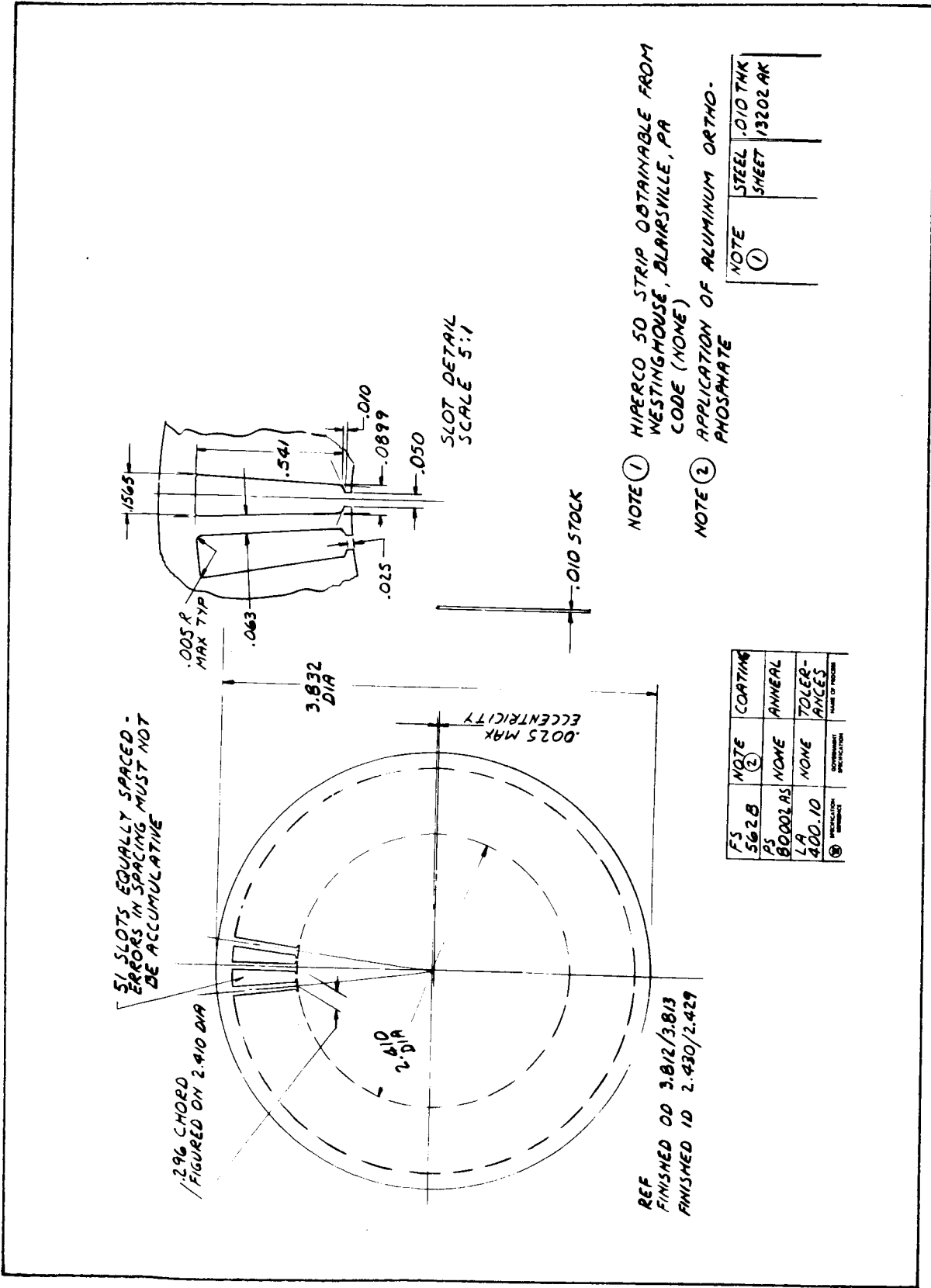


Figure 1. Motor Armature Punching

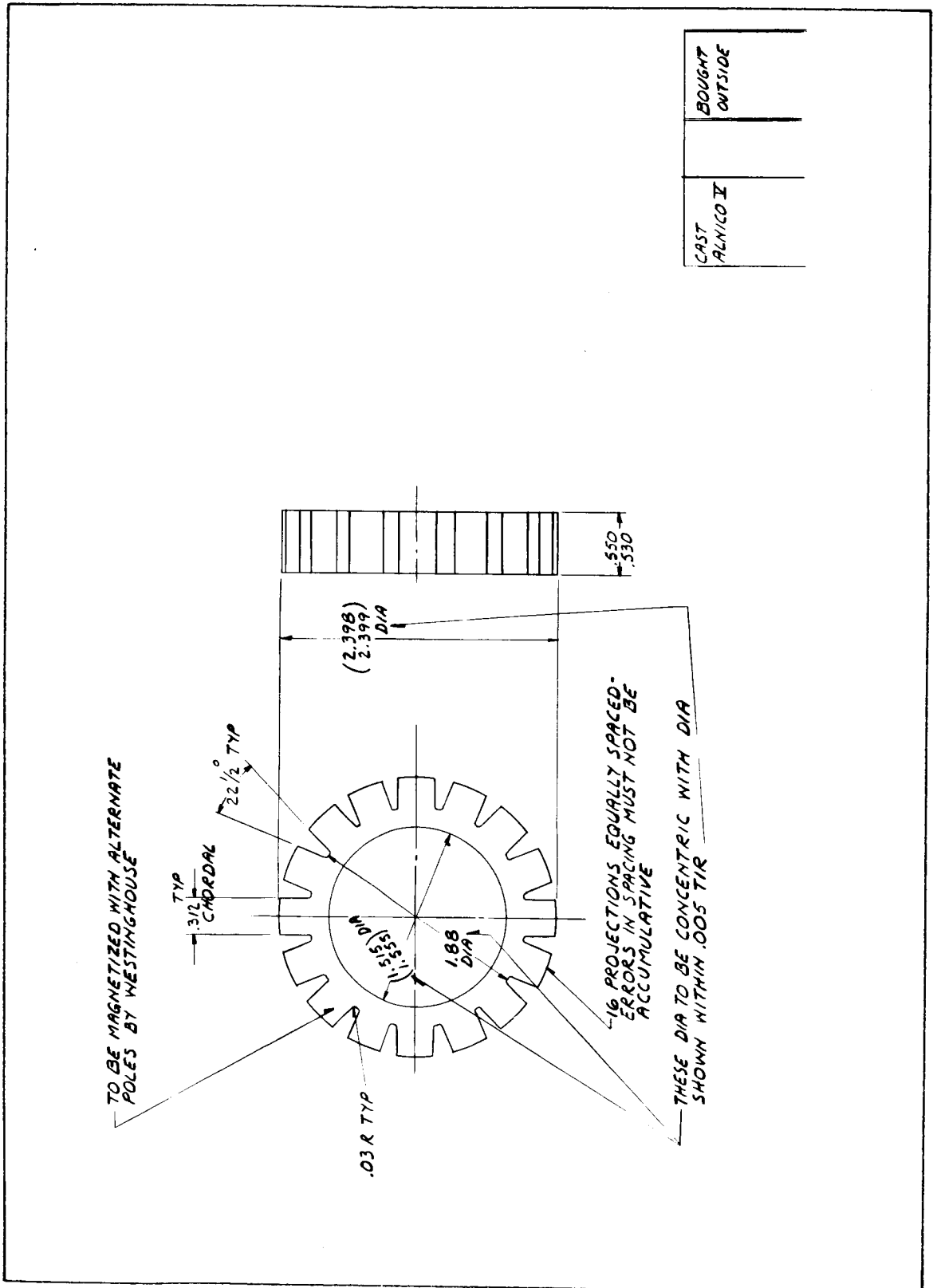


Figure 2. Permanent Magnet Rotor

Motor Core Length	0.53
Magnet Operating Flux Density	70,000
Magnet Operating MMF	480
Magnet Leakage Permeance per Pole	15.3
Air Gap Flux Density	49,500
Stator Tooth Flux Density	132,000
Stator Depth Below Slot Flux Density	70,700
Leakage Factor	1.286
Saturation Factor	1.09
Effective Air Gap Permeance per Pole	53.4
Air Gap Flux per Pole	9030
Stator Tooth Flux per Pole	8710
Slot Area Minus Insulation	0.053
Slot Fullness - Percent	67.0
Coil Throw	3 slots
Coil Perimeter	2.84
Turns per Coil	81
Total Number of Coils per Phase	17
Wire Size	#28
Total Series Conductors per Phase	2750
Cold Resistance per Phase	22.8
Assumed Winding Temperature	40°C
Total Circuit Hot Resistance	16.05
Total Effective Series Conductors	3770
Locked Torque - Full Voltage	95
No Load Speed - Full Voltage	150 RPM

TABLE 2. MOTOR DESIGN CHARACTERISTICS - Units are given in Table 1.

C. MAGNETIC SENSOR DESIGN

1. General Description

The magnetic sensor is depicted in Figures 3, 4, and 5. The basic purpose of the sensor is to provide rotor position (and rate) information suitable for brushless commutation and position and rate control of the torque motor shaft. The primary windings are excited by a 10 kc/s oscillator. The 10 kc/s flux generates voltages in the windings on the secondary teeth that are aligned with the rotor poles. The rotor of the sensor is mechanically attached to the motor shaft. Since the rotor position is sensed, position information is also available for control purposes. With proper design, a linear rising or falling pulse amplitude with position can be obtained for every position of the rotor on at least one of the six secondary windings. This information can be used for rate sensing at very low velocities. The rate sensing feature was originally conceived at NASA GSFC. Preliminary tests and extensive analytical results on the rate sensing are recorded in NASA GSFC Report No. X716-66-473 and Invention Disclosure No. D-1033.

2. Core Design

A preliminary design of the magnetic sensor core was given in the previous quarterly report. The final core shown in Figure 4 is identical except that the width of the teeth has been increased slightly to allow for tolerance and to assure overlap of the linear portion of the rate-sensing information from the six secondary windings. A summary of the design criteria is given below.

- (a) 16-Pole Design - Requires 6 secondary sensing windings in 45 degrees of rotation and 8 rotor poles.
- (b) Offset Tooth - In this type of design, only 3 secondary teeth are contained in 45 degrees. The remaining 3 teeth occur 180 degrees away, offset by one-half stator tooth pitch.
- (c) Parallel Groups - Teeth displaced by 45 degrees are positionally equal. One parallel group of teeth is added to the basic six with the tooth windings connected in series to obtain more secondary winding space.
- (d) Stator Tooth Width - Originally set equal to the slot opening. This theoretically gives a linear rising amplitude with position of at least one secondary output signal for every position of

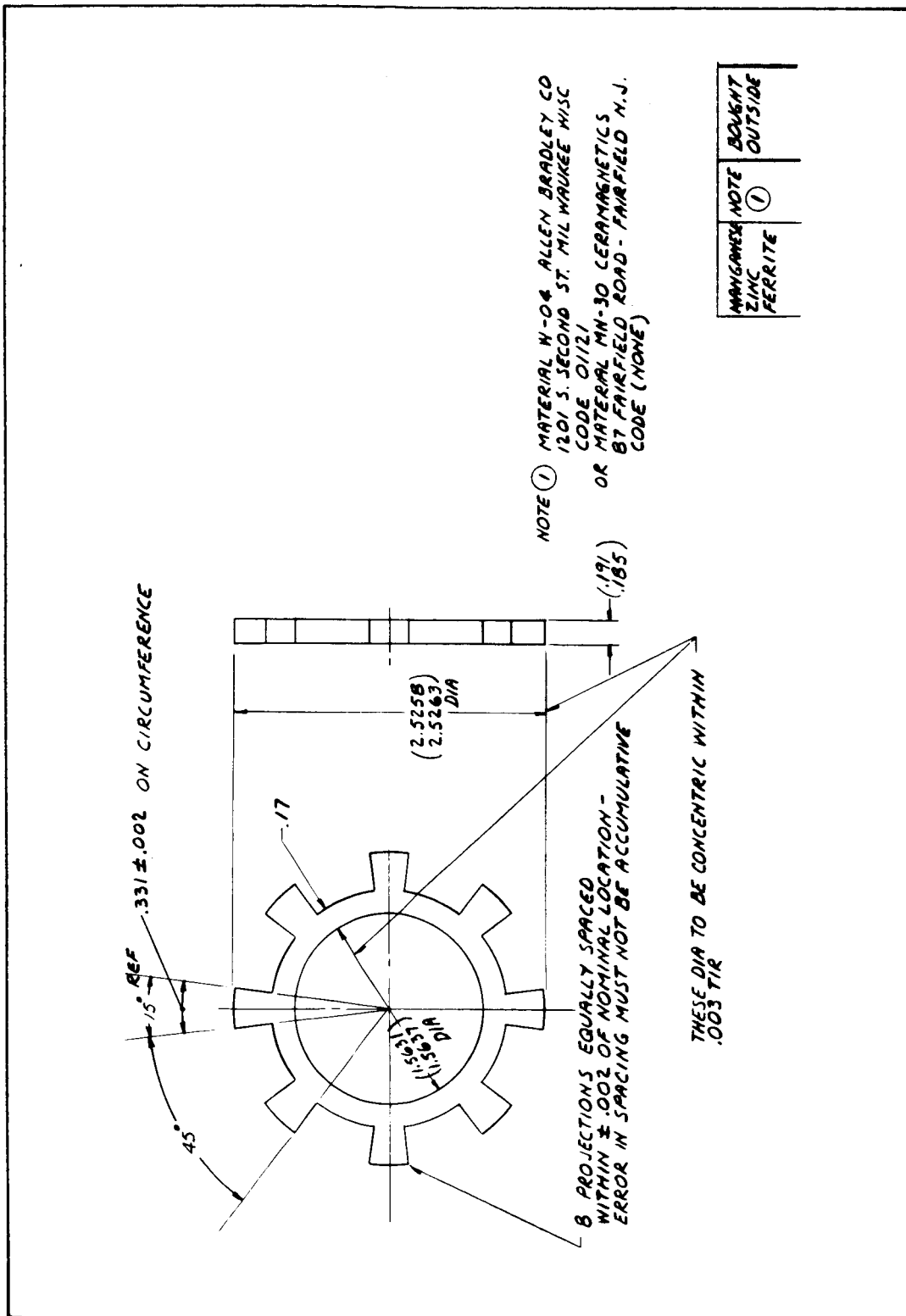
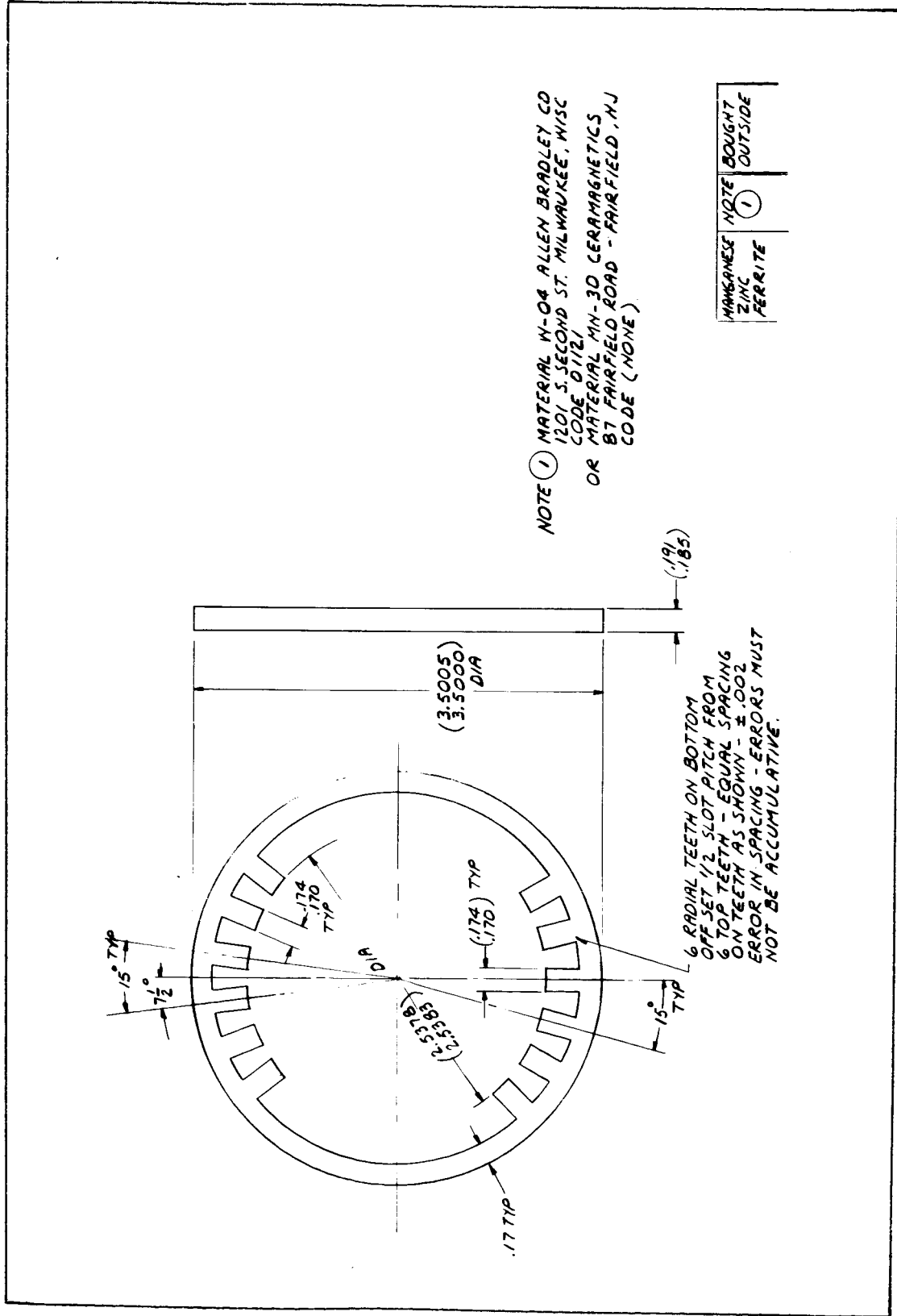


Figure 3. Magnetic Sensor Rotor Core



NOTE ① MATERIAL W-04 ALLEN BRADLEY CO
 1201 S. SECOND ST. MILWAUKEE, WISC
 CODE D1121
 OR MATERIAL MN-30 CERAMAGNETICS
 87 FAIRFIELD ROAD - FAIRFIELD, NJ
 CODE (NONE)

MANGANESE ZINC FERRITE	NOTE BOUGHT ① OUTSIDE
------------------------------	-----------------------------

Figure 4. Magnetic Sensor Stator Core

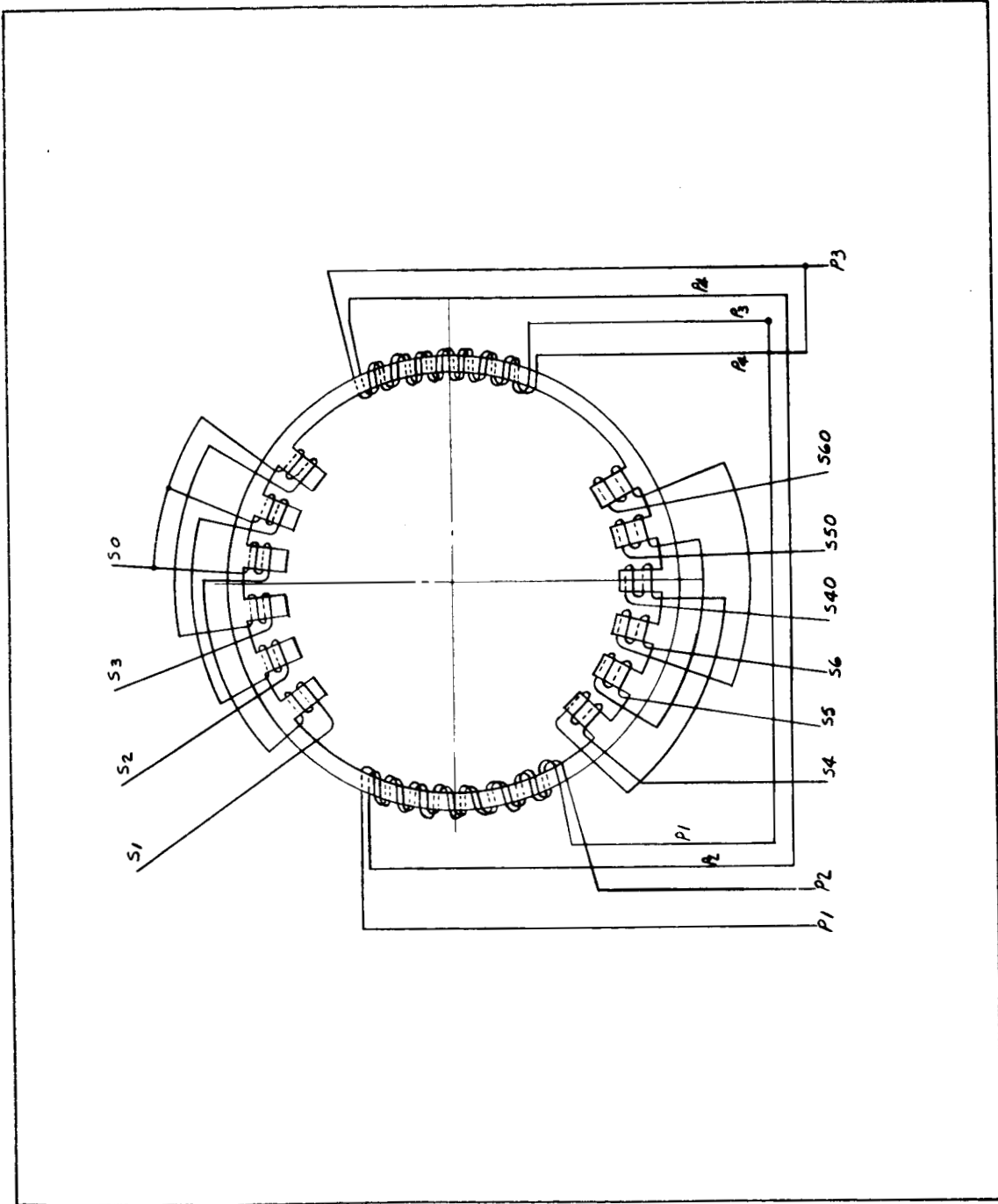


Figure 5. Magnetic Sensor Winding Diagram

the rotor. The width of the teeth was slightly increased in the final design to allow for tolerance and to assure overlap.

- (e) Rotor Pole Span - Set equal to one stator tooth pitch to give linearity to the rate sensing signal. This condition maintains a constant air gap permeance with rotation, giving zero cogging torque and minimizing the effect of leakage flux variations on linearity.
- (f) Other Parameters - Other dimensions of the sensor core were determined from the criteria of structural soundness, flux carrying capability, mechanical size, and minimizing flux leakage paths and electrical losses.
- (g) Material - Manganese Zinc Ferrite is used to obtain low core loss at the 10 kc/s cycling rate.
- (h) Air Gap - An air gap of 0.006 was considered to be the minimum practical gap.

3. Winding Design

General Description

The object of the design of the winding is to obtain a sufficiently strong device so that the output voltage amplitude is negligibly affected by the load current to be drawn by the circuit. Changes in load current will thus not affect the accuracy of the rate sensing information. It is desirable to accomplish this with the minimum size, weight, and electrical losses. Since the size and weight were practically determined by the core design, it is the function of the winding design to obtain minimum electrical losses. There is no set criteria for arriving at this minimum. The design procedure was to calculate the performance with windings of successively less strength until it was felt that any appreciable further reduction would compromise the rate-sensing function. To be conservative, the performance was calculated with a secondary load of 0.010 amps. The actual peak predicted load in the circuit is approximately 0.003 amps. It is intended in the design to obtain a 12.5 volt peak amplitude on the secondary with a 28 volt input to the primary.

Design

The first step in the design is to estimate the leakage and mutual permeances. This was done by a rough procedure using the methods of Roters'. Because of the complex leakage paths in the inner core

and on the ends, the estimation of leakage is necessarily approximate. However, because a trial and error design will later be made, it is felt that the procedure is adequate.

The total estimated leakage permeance for one-half of the total path on one side of the core is 14.10 of which 5.95 is intercore and 8.15 is end effect. The estimated mutual permeance (one tooth) is 21.7 of which 2.13 is end effect. The secondary slot leakage permeance (for one tooth) is 1.17 of which 0.59 is end effect. These permeances were for one particular position of the rotor. It is assumed that:

- (a) The leakage and mutual permeances do not change with rotor position.
- (b) The division between mutual and leakage flux is the same on the top as on the bottom of the sensor.
- (c) Partial linking of an inactive winding in the mutual path is regarded as mutual flux rather than leakage.
- (d) The circuit will be analyzed on a half-circuit basis. The two half-circuits are assumed to be equal.

The analysis using only a half-circuit can be visualized as though the core was cut in two down the vertical centerline. Since there are primary windings on both sides of the core connected in series, only one-half the primary voltage is applied to the half-circuit. The effective primary turns are those on one side only (1/2 the total). The total secondary turns are visualized as the sum of the turns on the top and bottom tooth. Although these are not connected, they are connected in series with a tooth in the other half-circuit, so the net result is the same when analyzing two fully linked secondary windings because the two half-circuits are identical. Thus the currents, resistance, voltage, and inductance are the same as though the two windings were connected in series.

The equivalent circuit for two fully linked secondary windings in the secondary on a half-circuit basis is shown in Figure 6. The symbols in the circuit are defined below.

- $V = 1/2$ applied line voltage (square wave peak)
- $R_p = 1/2$ of the total calculated primary resistance.
- $R_m =$ this value is derived from an estimate of the core loss and the fact that the half circuit must contain 1/2 the core loss

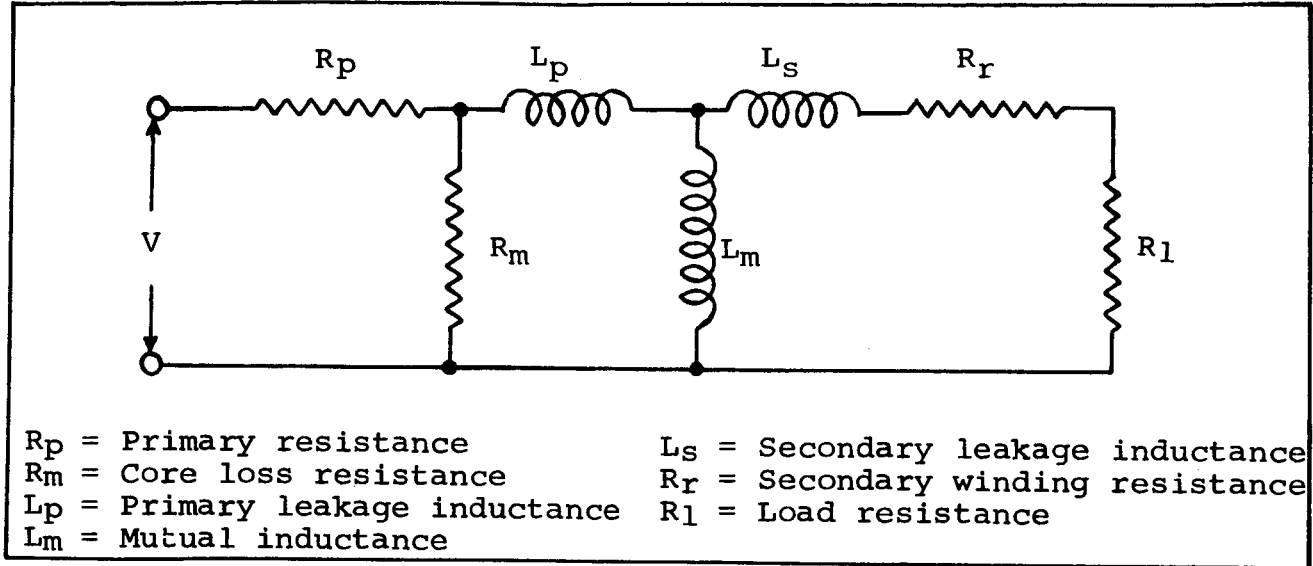


Figure 6. Equivalent Half-Circuit for Magnetic Sensor

$$\text{or } R_m = \frac{2 V^2}{\text{Core loss}}$$

L_p = Primary leakage inductance. The permeance used to calculate this is the permeance for one side of a half-circuit (value previously given) divided by 2 to obtain the permeance for both sides. Inductance is obtained by multiplying by $(\text{total primary turns}/2)^2$ (10-8).

L_m = Mutual inductance. Obtained same as above.

L_s = Secondary leakage inductance. This is the slot leakage only for two slots in parallel, one in the top and one in the bottom.

$$L_s = (2)(\text{primary turns}/2)^2(\text{one slot leakage permeance}) \quad (10-8).$$

T = Turns ratio. This is defined as $(\text{primary turns}/2)/(\text{secondary turns})$ where secondary turns are for 2 teeth windings in series.

R_s = Actual calculated secondary resistance for two teeth windings in series times T^2 to refer to primary.

R_l = Actual calculated load resistance times T^2 to refer to primary.

When the circuit is solved, the input current will be the actual primary current since the two half-circuits are connected in series on the primary side. Calculated losses will be one-half the total. The

secondary current will be the actual multiplied by T. The secondary voltage will be the actual divided by T. The analysis of the circuit on an incremental basis will determine the peak value of the fully coupled secondary voltage and the shape of the output pulse.

Although several iterations were made in the design, only the final design is given. The characteristics of the final design are given below in Table 3. The half-circuit constants are given in Table 4.

Primary Winding - 240 turns per side, center tapped, #22 wire, perimeter = 1.22
Secondary Winding - 89 turns per tooth, #33 wire, perimeter = 1.036
Leakage permeance (1/2 circuit) = 7.05
Mutual Permeance (1/2 circuit) = 10.85
Secondary (slot) Permeance (1/2 circuit) = 2.34
Primary Resistance (actual) = 0.444 ohms end to center tap
Secondary Resistance (actual) = 2.00 ohms (2 windings in series)
Stator Teeth Peak Flux Density = 5680 lines per inch squared
Stator Core Peak Flux Density = 9350
Rotor Teeth Peak Flux Density = 2840
Rotor Core Peak Flux Density = 9350
Peak Primary Flux = 292 lines
Core Loss = 0.284 watts

TABLE 3. MAGNETIC SENSOR DESIGN CHARACTERISTICS

$R_p = 0.222$
$R_m = 1380$
$L_p = 0.001014$
$L_m = 0.001560$
$L_s = 0.000337$
$R_s = 0.91$
$R_1 = 570$
$T = 0.675$

TABLE 4. MAGNETIC SENSOR HALF-CIRCUIT CONSTANTS

The primary and secondary winding resistances are so low and R_m so high that they may be neglected for an approximate solution. The approximate solution for secondary current when this is done is:

$$i_z = \frac{b}{a} (1 - e^{-at}) + i_0 e^{-at}$$

where i_z = secondary current
 i_0 = initial value secondary current
 t = time
 $b = \frac{L_m V}{L_p L_m + L_s L_m + L_s L_p}$
 $a = \frac{R_1 (L_p + L_m)}{L_p L_m + L_s L_m + L_s L_p}$

Solving this at $t = 1/2$ cycle of 10 kc/s = 0.5×10^{-4} sec

$$(1) \quad i_{z1} = 0.0149 (1 - e^{-29.9}), \quad i_0 = 0$$

$$i_{z1} = 0.0149$$

$$(2) \quad i_{z2} = -0.0149 (1 - e^{-29.9}) + 0.0149 e^{-29.9} = -0.0149$$

The analysis over the second interval shows this to be the steady state value with resistances neglected.

$$\text{Actual secondary current} = (0.0149)(T) = 0.01006$$

$$\text{Output voltage} = (0.0149)(R_1 / T) = 12.58$$

$$\text{The formula shows that the final current} = b/a = \frac{L_m V}{(L_p + L_m)R_1}$$

which indicates that the reactances act like a voltage divider same as they would at no load so that there is no difference between unloaded secondary voltage and loaded secondary voltage with resistances neglected.

$$\text{The drop in } R_p \text{ due to the load current} = (0.222)(0.0149) = 0.0033.$$

Referred to the secondary, this is 0.0049 which is negligible.

R_m takes $14/1380 = 0.01015$ amps which provides negligible drop in R_p . The effect of secondary resistance on voltage is obviously negligible because of its relative value with R_1 .

It is concluded therefore, that there would be negligible secondary voltage drop with 0.010 amps load on the secondary. The effect of the secondary load on voltage levels therefore, is negligible even at the half-linked point where circuit switching takes place.

The primary current can be determined by the following at the same time interval.

$$i_m = \frac{Vt}{2(L_p + L_m)} = \frac{(14)(0.5)(10^{-4})}{(0.02574)(2)} = 0.136$$

Total primary peak current = $0.136 + 0.0149 + 0.010 = 0.161$ amps with 0.010 amps actual secondary current.

The primary voltage = 14 volts which is $14/0.675 = 20.7$ volts referred to the secondary with 12.58 volts out. This means that 8.12 volts worth of flux is shunted into the leakage paths. By ratioing the permeance in the leakage path associated with flux that would link one uncoupled tooth to the total leakage times this voltage, the uncoupled voltage is obtained. This was equal to:

$$\left(\frac{3.829}{14.10} \right) (8.12) = 2.21$$

The difference between coupled voltage and the uncoupled voltage = 10.37 volts. An approximate value for the angle sensitivity can be obtained by dividing this value by the mechanical angle of the tooth face, taking approximately 90 percent of the value to allow for non-linearities at the beginning and end of the linear range.

$$\text{Angle sensitivity} = \frac{(0.9)(10.37)}{7.5} = 1.24 \text{ volts/degree.}$$

To obtain the shape of the fully linked output pulse, the circuit was solved incrementally on a digital computer. The plot of output voltage versus time is shown in Figure 7.

It is known that there is some variation in leakage permeance with rotor position. Consequently, there will be some variation in output voltage between different secondaries which will cause a variance in the angle sensitivity. It is considered necessary to perform a trial and error design of the sensor to adjust the turns on each tooth for equal voltage. This will be performed as soon as a core is available in the next quarter.

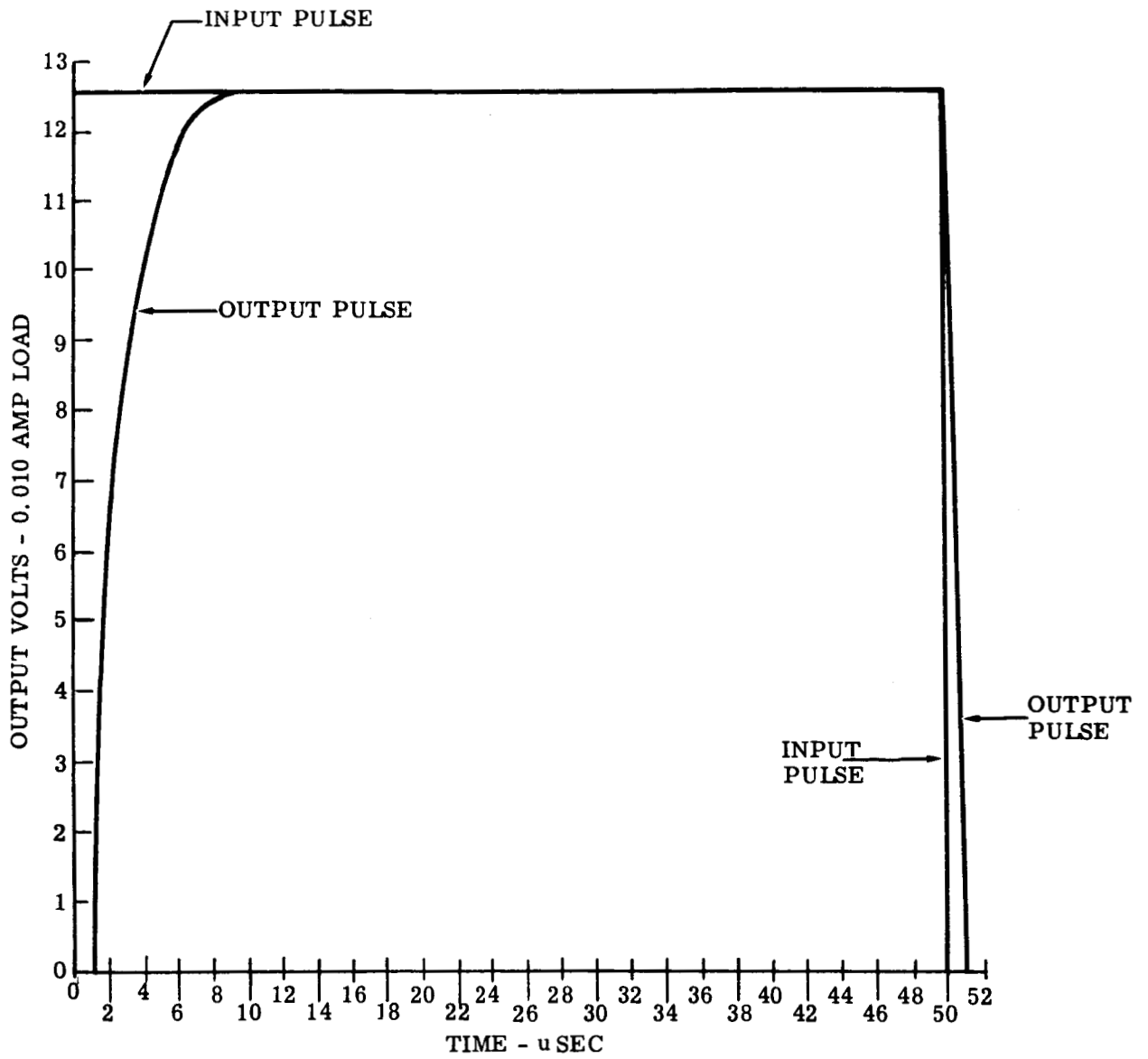
D. CONTROLLER-COMMUTATOR CIRCUIT DESIGN

1. General Description

The circuit provides the functions of commutation, speed control, reverse-ability and stand by operation. The theory and operation of the circuit was described in the previous quarterly report and a complete circuit schematic was provided. This part of the previous quarterly report is included in Appendix I.

2. Circuit Changes

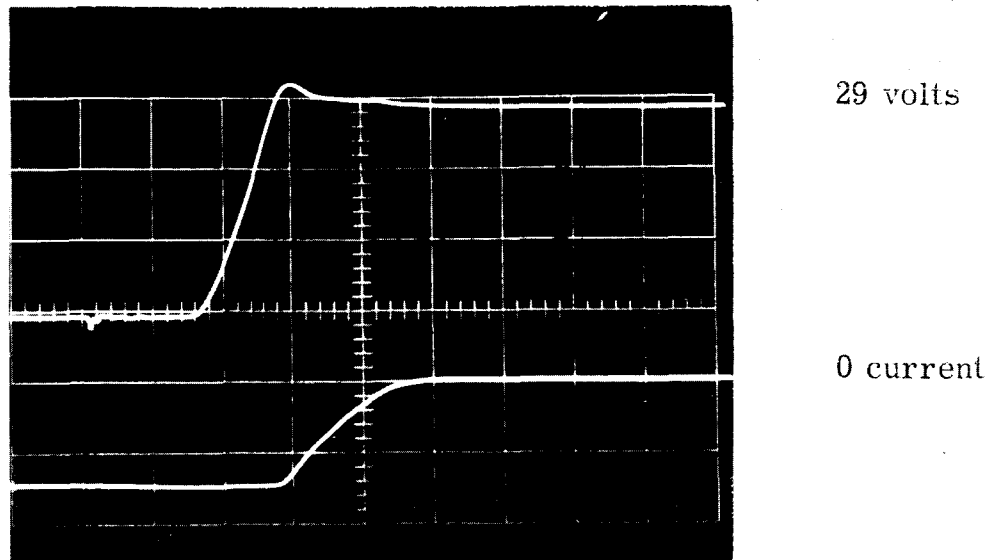
In the circuit previously given, the top row in the transistor bridge was used for pulse-width-modulation, turning on and off at a 10 kc/s rate. The bottom row was kept continuously on with a capacitor filter of the drive. Because of the circuit configuration, the top row transistors are necessarily PNP transistors. At the conception of the circuit, it was felt that high-speed PNP transistors could be obtained. However, a canvas of suppliers determined this to be untrue. Tests were taken on one of the best available PNP transistors to determine switching losses at the 10 kc/s rate. Superimposed traces of current and voltage drop in the transistor with a simulated inductive load revealed the phenomena that the full current is maintained thru the transistor almost to complete shutoff. A picture of these oscillograph traces is shown in Figure 8.



DATA FOR OUTPUT PULSE

<u>TIME</u>	<u>VOLTS</u>
1	0
1.25	2.49
1.75	4.99
2.6	7.51
4.0	10.0
9.5	12.58
50.0	12.58
51.0	0

Figure 7. Fully Linked Output Voltage Pulse Versus Time



Time progresses left to right
 Top trace - Voltage drop across transistor
 Bottom trace - Current through transistor
 Time Scale = 1 usec/cm
 Line Voltage = 28 volts

Figure 8. Switching Characteristics with Inductive Load -
 PNP Transistor 2N3201

The explanation of the action lies in the fact that the current cannot transfer to the commutating path until a reverse voltage across the commutating path is attained. This does not happen until the voltage drop across the transistor rises to above line voltage. The tests demonstrated that excessive switching losses would occur if the pulse width modulation was attempted with the slow PNP transistors.

It was therefore necessary to pulse-width modulate the bottom row transistor and to keep the top row switches on continuously. The basic operation of the circuit is the same except that the pulse-width-modulation was transferred to the bottom row switches and the capacitor delay was transferred to the top row switches. Several components had to be added and some circuit changes made to accommodate the the new configuration. A complete circuit schematic of the revised circuit is given in Figure 9. The above change and other circuit refinements resulted in the addition of 16 components for a total of 132 counting the Schmidt triggers as one component.

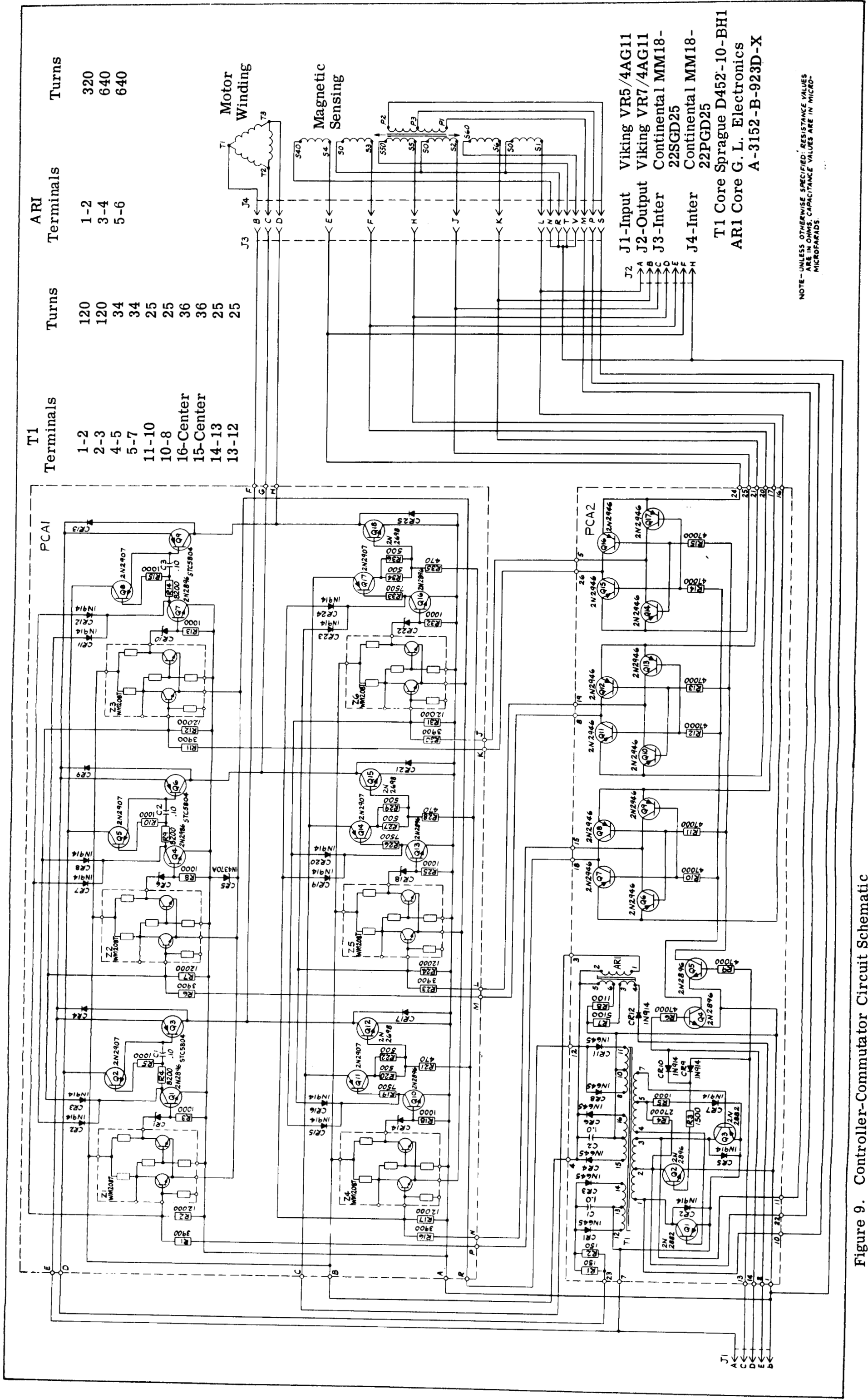


Figure 9. Controller-Commutator Circuit Schematic

3. Design

The derating practices given in Table 5 were followed as a minimum in the design.

Resistors - 20% on power
Capacitors - 50% on voltage
Transistors - 50% on voltage - 30% on current
Diodes - 40% on PIV, 50% on current
Zener Diodes - 20% on power
Schmidt Triggers - 70% on voltage

TABLE 5. SOLID STATE COMPONENT DERATING PRACTICE

Component values were selected and their operation verified in the final breadboard of the circuit. The final values selected plus the part numbers of the solid state devices and connectors are shown on the schematic of Figure 9. The main power transistors are heat sunked for vacuum operation.

All the solid state devices used are silicon. Resistors are carbon composition and wire wound. Capacitors are solid electrolyte (tantalum). Transformer cores are either Hi-Mu 80 or Orthonik with phenolic core boxes wound with DuPont ML enamelled wire which has high temperature capability (in excess of 200°C). The transformers are potted in silicone potting compound. The printed circuit boards are epoxy glass with silver plated terminals. Teflon insulated lead wire is used for interconnections. Corrosion resistant hardware, either stainless steel or beryllium copper is used throughout. The aluminum container is chemically filmed per MIL-E-5541.

Connectors compatible with a space environment were selected. The five pin input connector contains terminals for the forward and reverse signals, the speed control voltage, and the line voltage. The seven pin output connector contains terminals for the rate and position information from the magnetic sensor. All connections to the connectors are shown in the Schematic.

E. MECHANICAL DESIGN

1. General Discussion

The unit is designed so that the control circuit package and the motor-sensor package are combined with the control package mounted on the end. However, the control can be separated and the two components operated separately if a jumper cable is used. The magnetic sensor stator is permanently mounted in the end bell. Adjustment is accomplished by rotating the end bell. Adjusting slots are provided in the end bell for the mounting screws.

2. Manufacturing Procedure

A cross-sectional view of the motor controller is given in Figure 10. The various major parts are identified on the drawing.

Motor Stator

The armature punchings are annealed and treated with aluminum orthophosphate for insulation. The punchings are then bonded together with epoxy cement. The core is wound, dipped and baked and machined. The bore can is inserted (shrink fit) into the bore which is then re-machined. The frame is heated to allow insertion of the wound core which has an interference fit.

Motor End Bells

The end bells are rough machined from bar stock. Knurled stainless steel inserts are pressed into the bearing housings. The end bells are then finish machined, treated with chemical film, and a gold flash is given to the inserts.

Magnetic Sensor Stator and Rotor

The completely machined cores are bought outside (Ceramagnetics, 87 Fairfield Road, Fairfield, New Jersey). End punchings of 0.031 inch thick Doryl-glass laminate are glued in place with a silicone adhesive. The stator is wound and dipped and baked. The stator is then mounted permanently in the right end bell.

Rotor Assembly

The shaft is machined from bar stock. The sensor rotor and permanent magnet are then mounted on the shaft against the inner shoulders. The sensor rotor sides are coated with Doryl varnish.

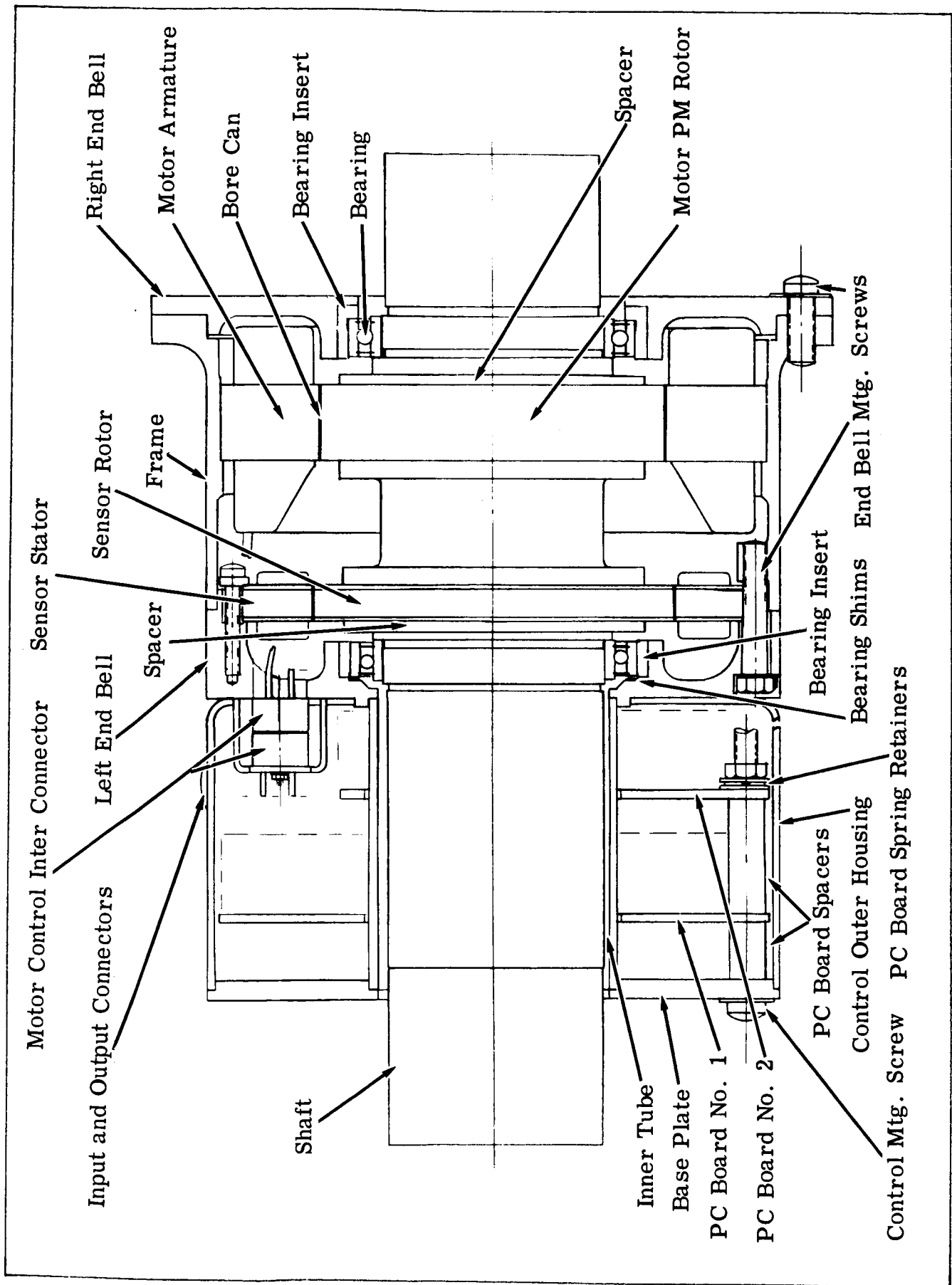


Figure 10. Mechanical Configuration

Spacers are pressed on against the two components. The permanent magnet is pinned in place through the interpolar gaps to the spacer and inner shaft shoulder. The pins are shimmed to provide a solid hold on the magnet and the shims coated with varnish to hold them in place. The varnish is cured and then the bearing journals qualified.

Motor Assembly

The rotor is temporarily inserted into the stator with the end bells mounted. The bearings have slip fits on both the shaft and housing. The proper number of shims in the right end bell housing is determined so that total rotor axial movement is limited to 0.004 to 0.006 inch with a two pound load applied axially in both directions. The unit is then disassembled. The rotor permanent magnet is magnetized with a keeper placed on the magnet. The unit is then reassembled with the keeper being removed during insertion of the rotor. Connections are made and the connector mounted to the motor.

Control Package

The circuit boards are connected and mounted to the base plate with the spacers and three mounting screws. The boards are held in the base-spacer assembly with a spring retainer against the mounting screws. The outer housing is placed over the assembly and connections made to the connectors. After the inner tube is inserted, the control is ready for assembly to the motor. This is accomplished by turning the mounting screws into threaded holes in the end bell. A pilot is provided on the end bell for locating.

3. Specific Comments

- a. Bearing System. The bearings to be used are Barden bearings, catalogue number A543SSTB. This bearing is a thin bearing with a large bore having a T-type retainer composed of glass fiber reinforced teflon filled with MoS_2 . This solid lubricant is a proprietary Barden material with the trade name of "Bar-Temp". Consultation with Barden engineering determined that this bearing has been used previously in space application and that it did not exhibit any severe "sticking" characteristic. Other characteristics also appear to be satisfactory for this application. The bearing is double shielded to prevent particle contamination.

According to Barden Engineering, this bearing is capable of continuously sustaining a radial load of approximately 10 pounds. Barden Engineering recommended that if preloading was used, it should be limited to one or two pounds. Because of the large diameter of the bearing and the unusually light force required, it would be quite difficult to obtain a spring to accomplish the preload. Also, because of the low speed, preloading was not considered necessary. Consequently, no preload is used on the bearings. The axial clearance in the housing is taken up with shims until a movement slightly above the expected axial free play in the bearing is obtained. The bearing free play is greatly in excess of the differential thermal expansion of the frame and shaft over the temperature range. The bearings have a slip fit on the shaft and in the housing. The bearing inserts are gold-plated to prevent cold-welding of the bearing to the housing in a vacuum.

- b. **Structural integrity of Sensor Cores.** The structural integrity of the ferrite cores is enhanced by cementing 0.031 inch thick punchings of Doryl-glass laminate on the core sides. These punchings have the same shape as the cores. The Doryl-glass laminate, produced by Westinghouse, is a high temperature, low outgassing material with high structural strength. The flexural strength, which is the characteristics of most interest in this purpose, of the laminate is in excess of 70,000 psi. This compares with a flexural strength of most epoxy coatings of approximately 12,000 psi. The cement used is a silicone varnish which in the past has given the most satisfactory results in cementing end punchings to stator cores. The varnish, a thin fluid when uncured, gives its adhering properties with a very thin film.

4. Weight Estimate

The total estimated weight of the motor-controller is 4.7 pounds. This is broken down as follows:

Motor electrical weight	- 1.45
Magnetic Sensor weight	- 0.28
Shaft and Spacers	- 0.86
Frame and End Bells	- 0.98

Circuit Package - 0.80
Miscellaneous - 0.33

Total - 4.70 pounds

5. Materials and Finishes

A complete list of materials used in the motor-controller excluding the printed circuit boards, circuit components, and connectors, is given in Table 6. All aluminum parts used are given a chemical film per MIL-C-5541. All other parts used are inherently corrosion resistant and are given no surface treatment for retarding corrosion. No paint is applied to the unit.

F. OPERATING CHARACTERISTICS

1. Physical Configuration

The physical configuration, connector inputs, and connector part numbers are given in Figure 11. The total weight of the unit is 4.7 pounds.

2. Forward, Reverse, and Standby

The forward and reverse voltage connection to the input connector is shown on Figure 11. The operation is such that if a 15 volt d-c signal is applied to the forward terminal and none to the reverse terminal, the motor will rotate in one direction. If this voltage is removed and applied to the reverse terminal, the motor will rotate in the opposite direction. If the voltage is removed from both terminals, the motor will be in a stand-by condition. No current will be drawn and the circuit will be completely idle. The motor will provide no torque in this condition. The impedance offered in the circuit to the voltage is 1500 ohms. Voltage should never be applied simultaneously to the forward and reverse terminals. Circuit damage would result if this is done since tandem transistors in the bridge would be driven on, resulting in a direct line short through the transistors. The circuit will operate satisfactorily with an input voltage from 12 to 18 volts.

3. Speed Control

The input terminal for the speed control voltage is also shown on Figure 11. A variable voltage from 0 to 15 volts applied at this point will control the speed of the motor. With zero or negative voltage applied, there will

Item	Material	Govt. Spec.	Supplier and Identification
Leads 19/0.003	Teflon Insulated	MIL-W-16878, Type E	
Brg Inserts, Spacers, Shaft	303 SST Bar	QQ-S-763, Class 303, COND A CD	
Stator Slot Wedges	Silicone-glass Laminate	MIL-P-997, Type GSG	
Stator Pchg. Bond	Epoxy Cement	--	EIP-REZ 510 Jones Dabney
Slot Insulation	ML Resin Treated Glass Cloth	--	Pyre ML, DuPont
Insulating Tape	ML Resin Tape		EE 6379, Permacel Tape Corp.
Magnet Wire	ML Resin Enamel	MIL-W-583, CL220, Type M3	
Lead Connection	Brazing Alloy	QQ-S-561, Class 3	
Sensor End Pchgs.	Glass-Doryl Resin Bonded Laminate	--	Doryl Laminate, Westinghouse
Stator Bore Can	50% Nickel Steel	--	Hipernik, Westinghouse
Stator Punching	Cobalt Steel	--	Hiperco 50, Westinghouse
Stator Pchg. Insulation	Aluminum Orthophosphate	--	--
Permanent Magnet	Cast Alnico V	--	--
Sensor Core	Manganese-Zinc Ferrite	--	MN-30, Ceramagnetics
Sensor End Pchg. Bond	Silicone Varnish	MIL-I-24092, Type M, Class 200	
End Bells, Frame	Aluminum Bar	QQ-A-225/6 T4	
Shim Brg. Housing	Beryllium Copper	QQ-C-533, COND 1/2H	
Shim - PM Shaft Pins	Copper	QQ-C-576, CR Soft Temper	
Sensor - Lock Plate - Control Housing	Aluminum	QQ-H-250/8 H34	
Connector Spacer	Stainless Steel	QQ-S-763, CL 416, COND A, CD	
PC Board Spacer	Glass-Plastic Tube	MIL-P-79 Form TR, Type GMG	
Control Housing Tube	Aluminum	QQ-A-225/5 T4	
Control Housing Cover	Aluminum	QQ-A-318B Condition Half Hard	
Lacing Tape	Teflon-Glass		Warren Wire Co.
Insulating Varnish	Doryl Resin		Doryl B109-3, Westinghouse
Hardware, Lockwire	Stainless Steel		
Solder - Connector	Pure Tin Solder	MIL-S-6872	
Flux	Flux	MIL-F-4995, Type I	

TABLE 6. MATERIAL LIST

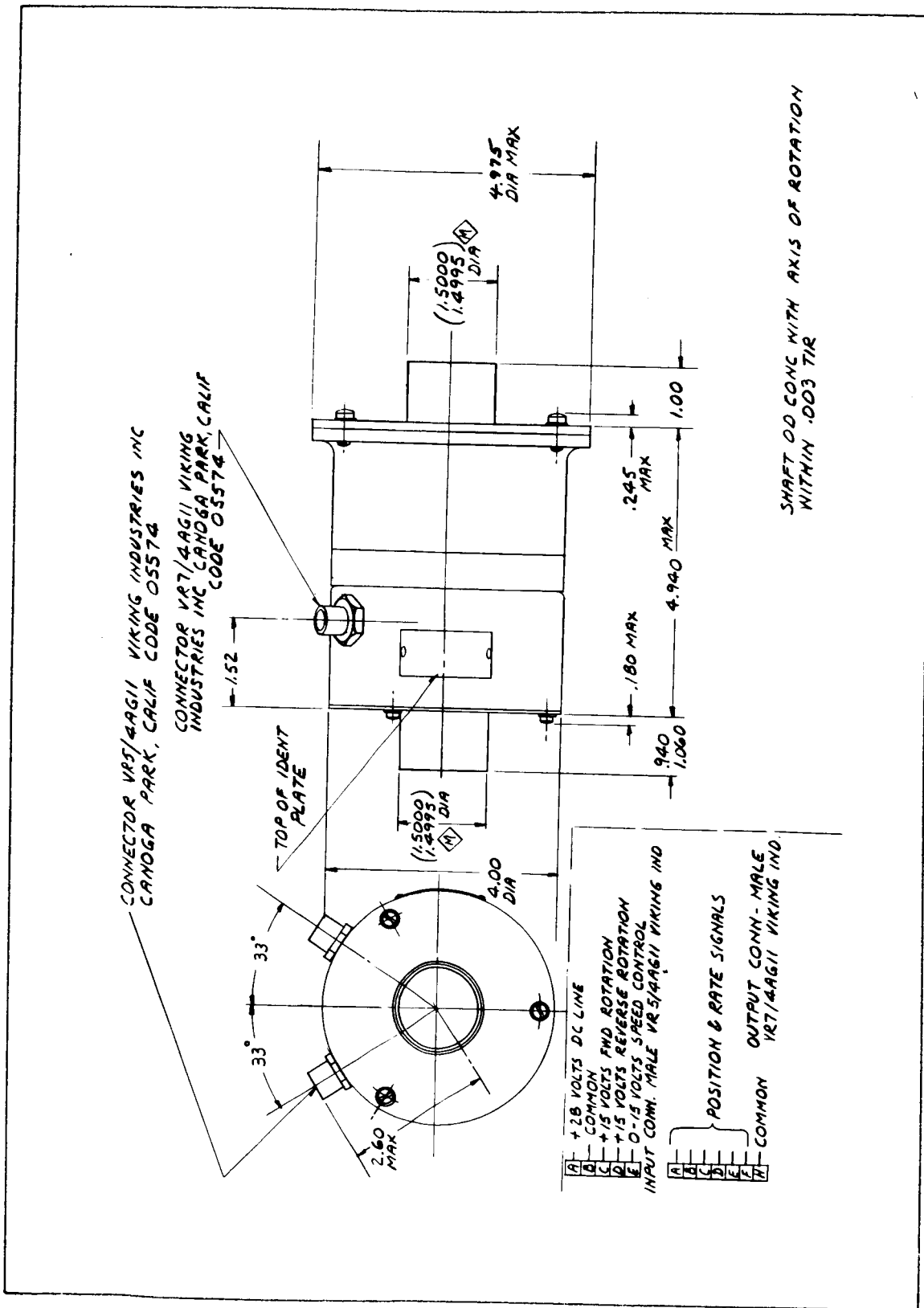


Figure 11. Motor Controller Outline

be no voltage applied to the motor and the motor will be idle. However, current will still be drawn in the logic portion of the circuit. With 15 volts or higher applied, the motor will be driven at half line-voltage since the maximum pulse width gives a 50 percent duty cycle. This is the maximum speed attainable.

The ideal curve of pulse width versus input signal voltage is shown in Figure 12. Superimposed on this curve is an actual curve taken on a test circuit using the same methods of control. This curve should be regarded as typical. The actual curve may deviate from this somewhat due to different component values. The linearity of the curve breaks down at the ends because of the inability to obtain a completely square loop material for the saturable reactor through which the control is accomplished and the inability to obtain the end points exactly.

The calculated full-voltage speed torque curve for the motor is shown on Figure 13. Also shown on this figure are a family of curves at different speed control voltages. These are obtained by ratioing directly with the effective applied voltage as determined by the pulse width obtained from the test curve of Figure 12. Since the motor requires a little voltage to overcome its own circuit drops and residual friction, no operation can be expected below a pulse width of approximately nine percent or a signal voltage of two volts.

These curves are shown for a 28 volt line voltage. If line voltage varies, the speed can be expected to follow the variation, but not directly except at full speed. Some compensation is obtained because a constant bias is provided the saturable reactor from the line and the variation in bias with line voltage will tend to compensate for the variation in voltage to the motor by varying the percentage pulse width. The compensation is not complete because part of the bias is supplied by the speed control signal which presumably remains constant. The amount of compensation is also variable depending on the original operating point.

The curves shown in the figures must be regarded as typical. Since the final motor is not available for test at this time, the actual curves cannot be obtained. Some deviations from the typical curves can be expected in the curves obtained at final test.

The motor at full voltage will draw an average line current of 0.4 amps at locked rotor. This will drop to approximately 0.075 amps at no load. Average line current at a constant torque can be expected to vary directly with the pulse width except that a nearly constant current of approximately 0.065 amps will be drawn by the logic circuit.

<u>DATA TEST CURVE</u>	
<u>% PULSE WIDTH</u>	<u>CONTROL VOLTS</u>
47	13
42	9
37	7.5
32	6.5
27	5.5
22	4.5
17	3.5
12	2.5
7	1.25
0	0

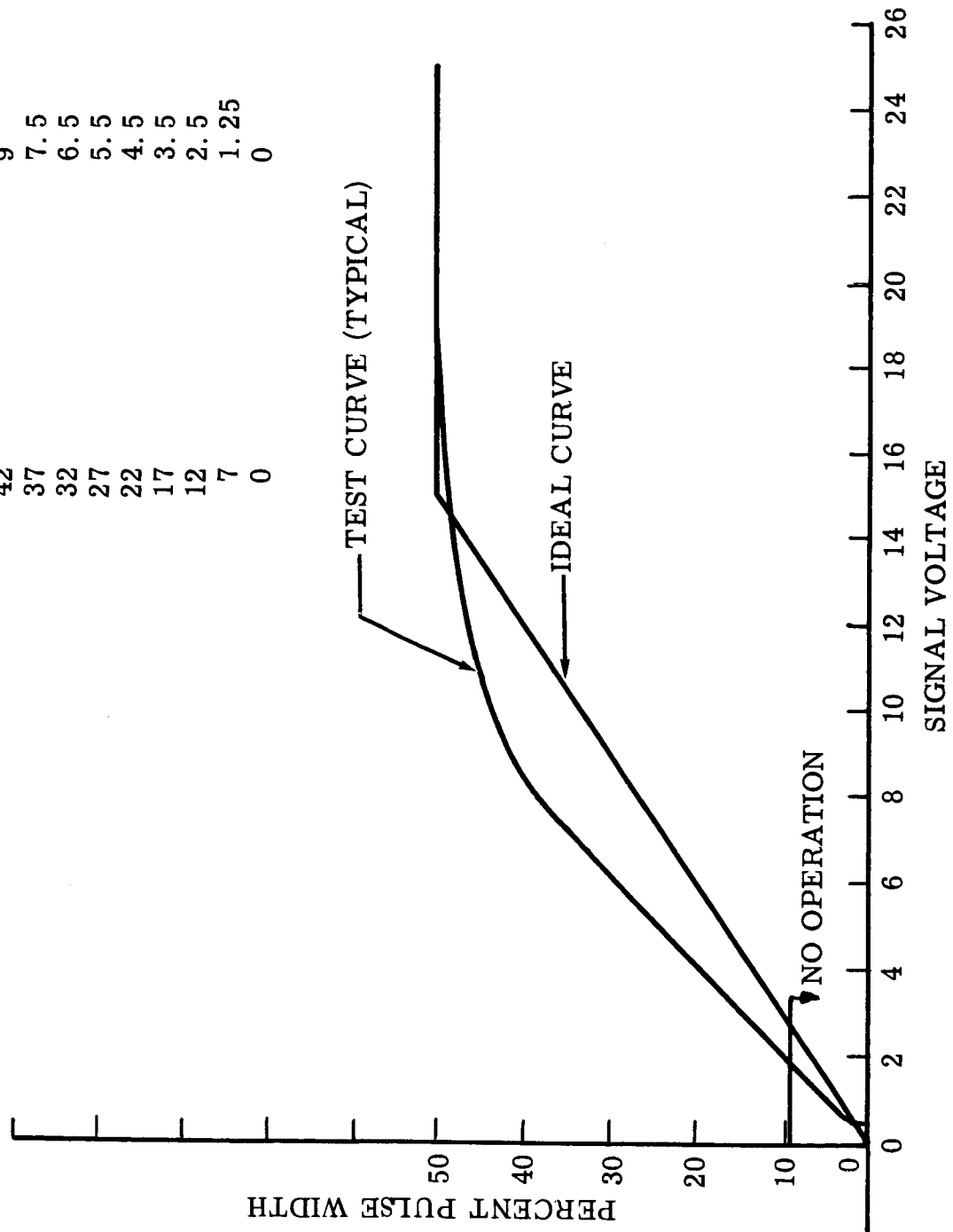


Figure 12. Pulse Width vs. Signal Voltage

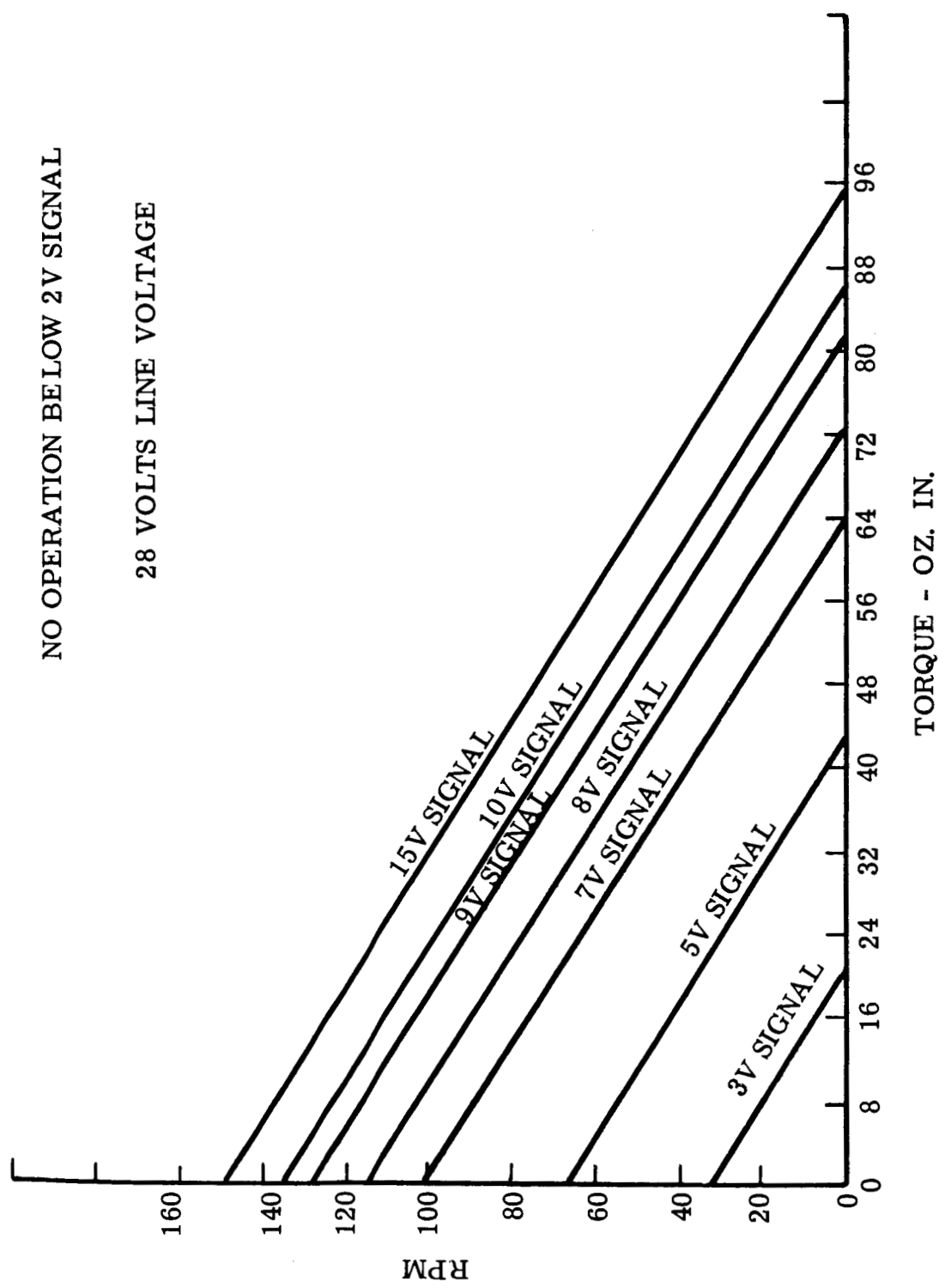


Figure 13. Calculated Speed Torque Curves vs. Speed Control Signal Voltage

Another source of variation in the speed-torque curves is the temperature of the winding. Variation in winding temperature will cause variations in the slope of the speed-torque curve. The locked torque will vary inversely with the resistance of the winding while the no-load speed will remain practically constant. The calculations were performed at a constant winding temperature of 40°C, which is the expected temperature at locked rotor and full voltage under room conditions with no conductive or forced cooling. The operating ambient temperature range is given as -10 to 70°C. The heat factor (multiplier on resistance at 25°C) at 40°C is 1.058. The heat factor at -10°C with a 15°C rise is 0.924. The heat factor at 70°C with a 15°C rise is 1.24. Therefore, the locked torque will vary from approximately 1.15 times the 40°C value in a -10°C ambient temperature to approximately 0.85 times the 40°C value in a 70°C ambient. These figures are based on having a 15°C winding temperature rise. The actual rise during operation in space would depend on the method of mounting used and the heat conducting area. It would also vary with the motor loading and pulse width. The temperature effects on the magnet are negligible compared to the effect on the winding.

The impedance offered by the circuit to the speed control voltage is 5100 ohms.

4. Rate and Position Information

The six secondary windings of the magnetic position sensor plus a common lead are connected to the output connector as shown on Figure 11. These six connections contain continuous position information. The type of information present on each secondary is shown in Figure 14 for a small angular rotation. This figure pictures the expected configuration of one amplitude envelope pulse. The rise in amplitude with position is linear for approximately 7.5 degrees. A plot of the positive half of the amplitude envelope pulses versus position for all six lines is shown on Figure 15. It is noted that the linear rise or fall portions of the amplitude envelope pulses overlap in the six lines so that for any position there is at least one line with a linear increasing amplitude. The linear regions could be utilized to continuously sense velocity at extremely low rates.

If line voltage varies, the amplitude of the pulses will vary almost directly with the line voltage. The frequency will also vary directly with the line voltage since a magnetic oscillator is used. The pulse width varies inversely with line voltage. Therefore, in the linear region of the pulse amplitude envelope the volt-second integral of the pulses will be almost constant at a given position regardless of the line voltage variation.

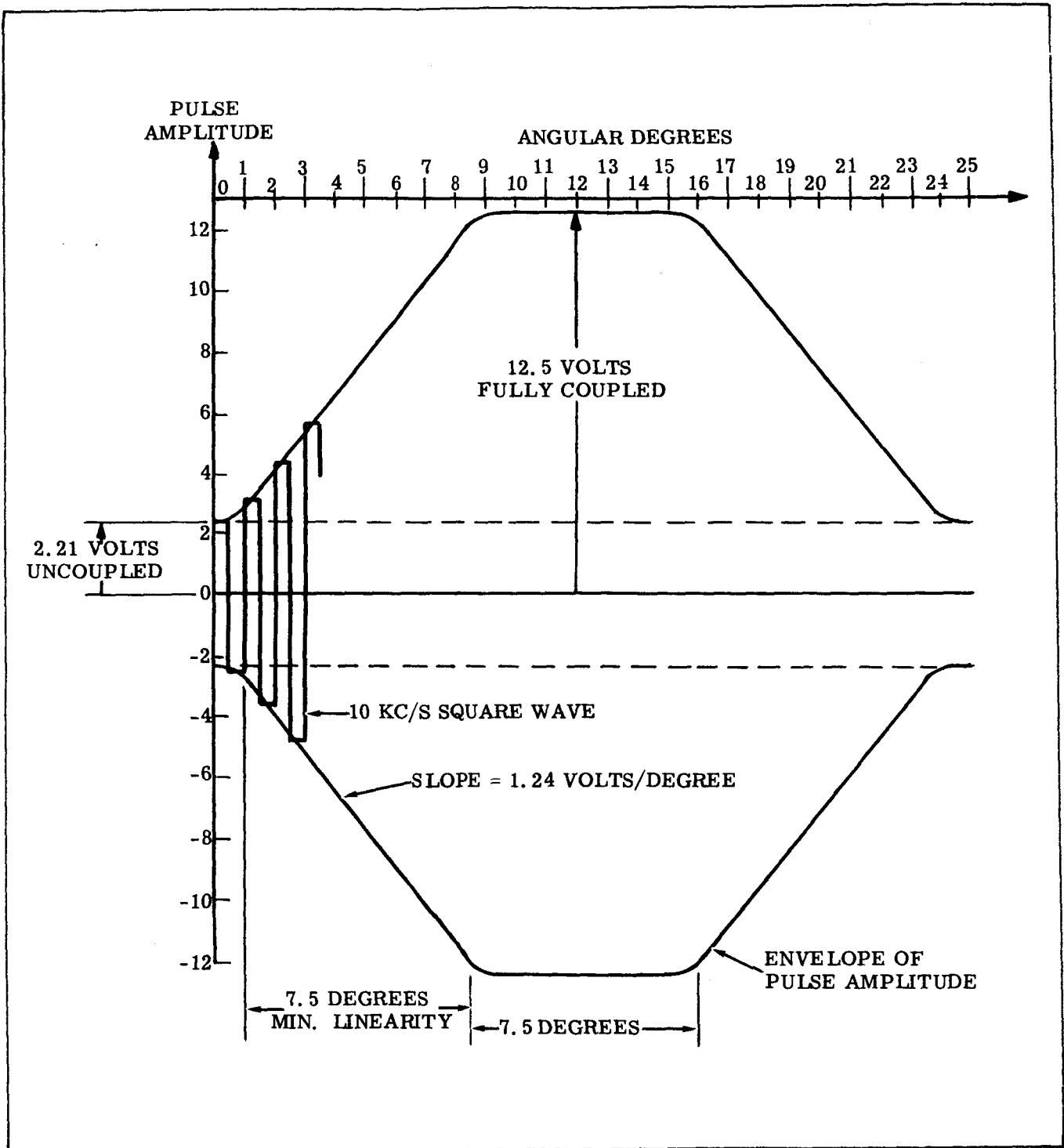


Figure 14. Detail of Amplitude Envelope Pulse

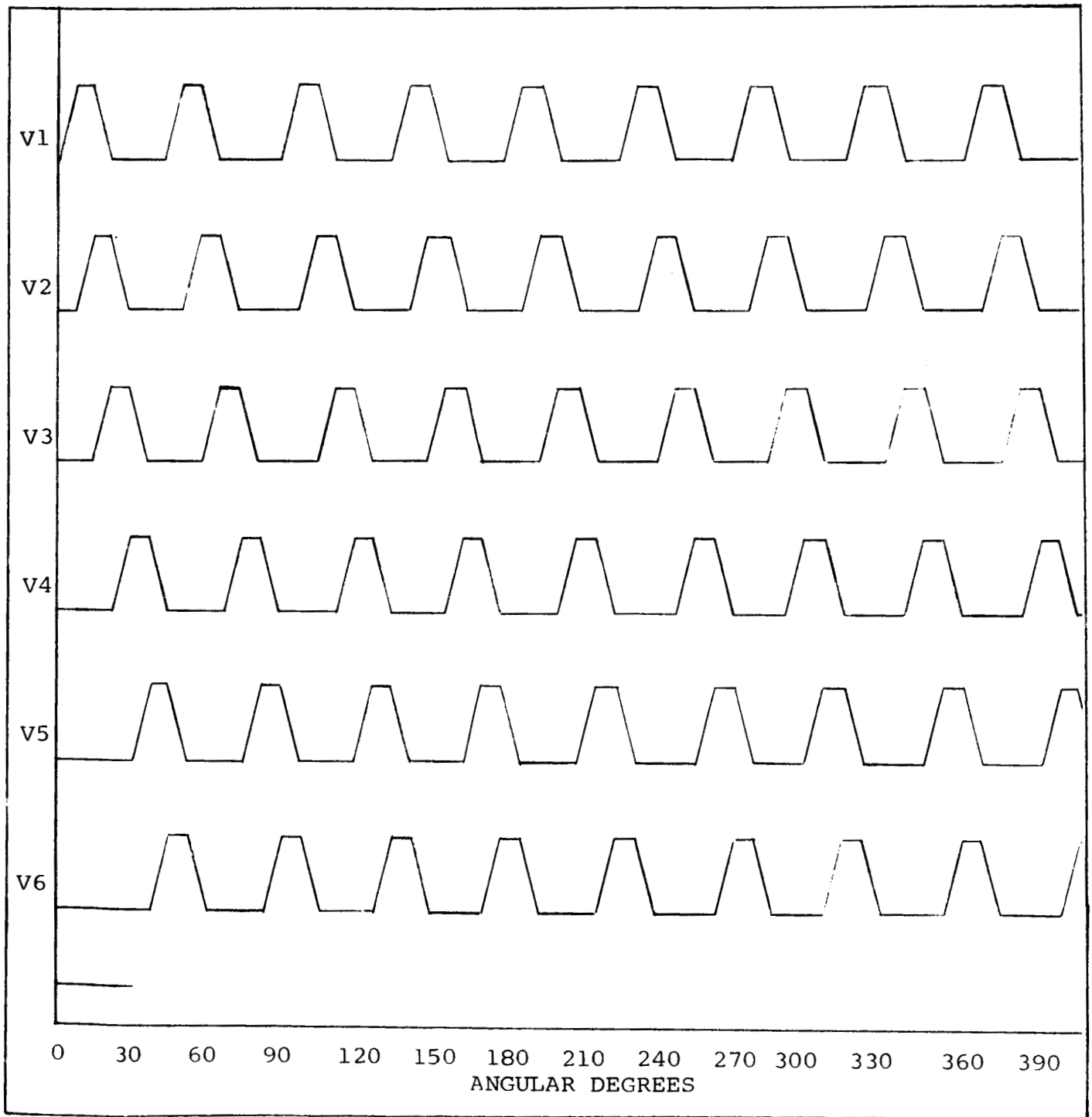


Figure 15. Amplitude of Sensor Output Signals Versus Angular Position

The sensor has an output capability of at least 0.010 amps without affecting the pulse amplitude significantly. The motor commutating circuit uses approximately 0.003 amps of this capability.

The position information as given above is calculated. The actual shape of the pulse amplitude envelope and the fully coupled and uncoupled amplitudes will be determined by test as soon as sensor cores are available.

G. TESTING PROCEDURE

The following test procedures will be followed when units are available.

1. Design of Magnetic Sensor

Obtain a magnetic sensor stator and rotor core when available. Glue on the end punchings if available. Wind stator core per drawing except do not dip and bake, tape coils or attach leads. Mount the stator and rotor core in the bearing and shaft system fabricated in the Research room.

Design

Move the rotor until a rotor pole is exactly centered under a stator tooth. Drive the sensor with the breadboard oscillator excited at 28 volts. Using an oscilloscope, determine the amplitude of the output pulse on the winding associated with that particular tooth. Repeat this for all six stator teeth positions. Adjust turns on the teeth until all secondary pulse amplitudes are equal at 12.5 volts.

Rate Sensing

After the above design adjustment, attach the rotor to the hour hand drive of an electric clock with a second hand. Take readings of secondary pulse amplitude of all six secondary windings with the clock not energized. Energize the clock and allow the second hand to make two revolutions (two minutes on the time scale), this corresponds to 1.0 degree of movement. Stop the clock by removing power and again record pulse amplitudes. Repeat for a total revolution of 45 degrees (45 readings).

2. Engineering Tests

The following tests will be performed by engineering when the complete motor-controllers are available.

- a. Oscillator. Check the output waveform, frequency, and losses. Check the voltages of all secondaries.
- b. Magnetic Sensor. Check the output wave form and voltage level on all secondary windings.
- c. Reversing Bridge. Check operation.
- d. Schmidt Triggers. Check the firing level of the Schmidt triggers. Check the output voltage.
- e. Lockout. Check operation.
- f. Main Bridge Circuit. Check the operation, drive voltages, and the capacitor delay operation.
- g. Speed Control. Check operation.
- h. Control Losses. Record current input without motor operation.
- i. Rough Adjustment of Sensor. Operate the motor at no load. Adjust the sensor stator position until maximum speed is obtained.
- j. Operational Check. Check functioning of all circuits with motor operating. Determine the minimum and maximum range of input voltage. Do not exceed 34 volts peak input.
- k. Hi and Low Temperature Operation. With the control placed in temperatures of -10°C and 70°C , check the operation at the minimum and maximum voltage input.
- l. Forward Losses. Record the voltage drop across the bridge transistors.
- m. Rate Sensing. Reduce the speed of the motor until the motor stops. Attach the electric clock drive and check the pulse amplitude of two adjacent sensor secondary windings versus position.

3. Laboratory Tests

Three units will be received from manufacturing. These units are to be submitted to engineering for circuit checkout prior to laboratory testing. When units are received in the lab from engineering, test per the following procedure. The units will be received with the control unit separate from the motor with an interconnecting cord.

- a. Resistance. With the control disconnected, measure and record the resistance between the following pins of the motor connector.

	<u>Cal. Value Ohms</u>		<u>Cal. Value Ohms</u>
<u>B</u> <u>C</u>	15.2 Motor	<u>E</u> <u>N</u>	1.8 Rel Sw Sec
<u>C</u> <u>D</u>	15.2 Motor	<u>F</u> <u>R</u>	1.8 Rel Sw Sec
<u>D</u> <u>C</u>	15.2 Motor	<u>H</u> <u>T</u>	1.8 Rel Sw Sec
<u>M</u> <u>P</u>	0.40 Rel. Sw Prim L-CT	<u>J</u> <u>R</u>	1.8 Rel Sw Sec
<u>S</u> <u>P</u>	0.40 Rel. Sw Prim L-CT	<u>K</u> <u>V</u>	1.8 Rel Sw Sec
		<u>L</u> <u>R</u>	1.8 Rel Sw Sec

Record room temperature

- b. Run-In. Drive motors between 400 to 600 rpm for four hours. Do not impose thrust or radial load on the motor shaft during run-in. Engineer to inspect motors after run-in.
- c. Cogging or Break-Away Torque. Connect a small spring scale to shaft with tape. Pull on spring scale in a tangential direction. Record maximum reading on scale prior to breakaway. Expected value is less than three ounces.
- d. Magnetic Sensor Adjustment - Engineer to be Present. The magnetic sensor or reluctance switch stator is mounted in the end bell with the connector. Adjustment is accomplished by loosening the end bell mounting screws and turning the end bell relative to the frame. Adjustment slots in the end bell are provided.

Connect the interconnecting cable between the motor and controller-commutator circuit. Connect a d-c power supply (No. 1) capable of varying voltage between 15 and 35 volts to pins A and B, (positive to pin A) of the 5-pin connector.

Connect a d-c power supply (No. 2) capable of varying voltage between 0 and 20 volts to pins E and B (positive to pin E) of the same connector. Monitor d-c current from power supply No. 1. Provide a third power supply (No. 3) of 15 volts through a 1-pole double throw switch with the positive side going to either pin D or C through the switch and the negative side to pin B on the same connector. With power supply No. 1 set at 28 volts, No. 2 set at 15 volts and No. 3 connected in either position, energize all power supplies (in any sequence). The motor should turn at a speed of approximately 150 rpm. Loosen the screws on the

end bell sufficiently so that the end bell can be turned. Monitoring the speed, adjust the position of the end bell until maximum speed is obtained. Mark this position. Repeat for the opposite direction of rotation (switch in Line No. 3 in other position). Mark this position. Set position at a point halfway between marks if different.

Mount the motor in a V-block with a wood torque arm attached to the shaft. Lock the torque arm to a scale capable of measuring from 0 to 150 ounce-inch of torque in conjunction with the torque arm used. Observe previous direction of rotation. Energize all three power supplies. Monitor frame temperature with a thermocouple until stable. Adjust motor height until torque arm is level. Loosen the clamp on the V-block and turn the motor stator very slowly by hand recording the minimum and maximum torque excursions over 360 degrees. Check for dead spots and dither. Repeat for the opposite direction of rotation. Take temperature rise by resistance after shutdown of motor winding. Record line current.

Depending on the results, the engineer may request another adjustment procedure on the end bell, adjusting for a minimum torque variation using the above procedure. Tighten adjusting screws.

- e. Speed Torque Curves. Take speed torque curves at the following voltages by allowing the shaft to slip inside the torque arm, adjusting torque by tightening the torque arm on the shaft. Record current in Line No. 1. Measure speed with a strobotac or by counting revolutions with a stop watch. Record frame temperature at locked at time of reading. Keep torque arm level.

Motor No. 1

Test No.	Power Supply		
	<u>No. 1</u>	<u>No. 2</u>	<u>No. 3</u>
1	28 volts	15	Forward
2	28	13	↓
3	28	11	
4	28	8	
5	28	4	
6	28	Min. Running at no load	
7	28	15	
8	28	8	↓

<u>Test No.</u>	<u>No. 1</u>	<u>Power Supply No. 2</u>	<u>No. 3</u>
9	28	Min. Running	Reverse
10	21	15	Forward
11	21	8	↓
12	21	Min. Running	
13	34	15	
14	34	8	
15	34	Min. Running	

Motor No. 2

28 volts	15	Forward
28	8	↓
28	Min. Running	
28	15	Reverse
28	Min. Running	↓

Motor No. 3 - Same as Motor No. 2.

Note: Line current in the above will vary from approximately 0.075 to 0.6 amps.

SECTION III

NEW TECHNOLOGY

A patent disclosure has been written on the controller-commutator circuit developed on this contract. The disclosure will be submitted in the normal manner. No other disclosures are contemplated on the motor-controller.

SECTION IV

PROGRAM FOR NEXT REPORTING INTERVAL

During the next quarter, parts procurement and tooling will be accomplished. Manufacturing will not start until the succeeding quarter. The trial and error design of the magnetic sensor winding will be accomplished as soon as parts are available.

SECTION V

CONCLUSIONS AND RECOMMENDATIONS

1. The motor-controller has been completely designed with the exception of the trial and error design of the magnetic sensor winding. No major problems are anticipated in manufacture.
2. The circuit had to be changed to accomplish the pulse-width-modulation with the fast NPN transistors. Excessive switching losses would have been encountered if the relatively slow PNP transistors were used. Some circuit modification was necessary to make the change.
3. The final circuit contains 132 components. Sixteen components were added to the previous circuit for the above change and other circuit refinements.
4. The calculated weight of the motor-controller is 4.7 pounds.

SECTION VI

BIBLIOGRAPHY

1. Yates, W. W., Skamfer, R. E., Final Report for a Brushless DC Torque Motor, NASA Contractor Report, NASA CR-374, February, 1966.
2. Veillette, L. J., Offset-Tooth Magnetic Rotor-Position and Velocity Sensor, NASA Invention Disclosure D#1033 (unpublished)
3. Roters, Herbert C., Electromagnetic Devices, John Wiley and Sons, Inc. 1941
4. Manual 7, Design and Application of Permanent Magnets, Published by Indiana General Corporation, Magnet Division, Valparaiso, Indiana.
5. Veillette, L. J., NASA GSFC Report No. X716-66-473

SECTION VII

APPENDIX I

CONTROLLER-COMMUTATOR CIRCUIT DESCRIPTION-PREVIOUS VERSION

This portion is directly reproduced from the First Quarterly Report.

C. SOLID STATE CONTROL CIRCUIT

1. Functional Description

The commutator circuit, exclusive of the reluctance switch which is considered part of the motor, consists of six sub-circuits. These are:

- Oscillator
- Reversing Bridge
- Regenerative Triggers
- Commutator Bridge
- Lockout Circuit
- Pulse-Width-Modulator

a. Oscillator

The reluctance switch drive oscillator with auxiliary drive windings is shown in Figure 6. The added windings, plus the diodes, provide isolated d-c drives for the Schmidt triggers and armature switches.

Transistor Q16 is normally off until a gating signal is applied to the base circuit. When Q16 is off, the oscillator is disabled (in standby condition).

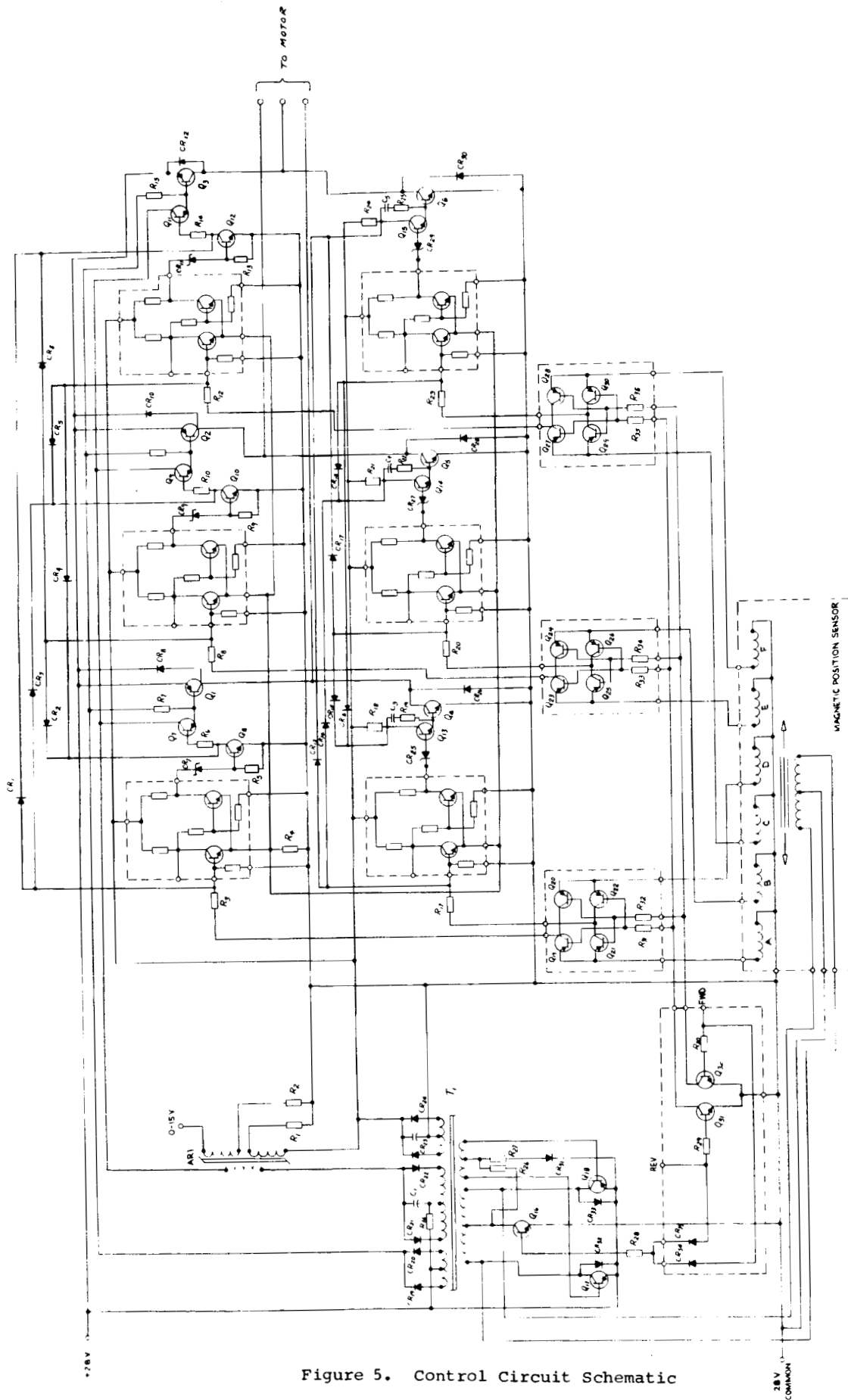


Figure 5. Control Circuit Schematic

WAED 66.51E-22

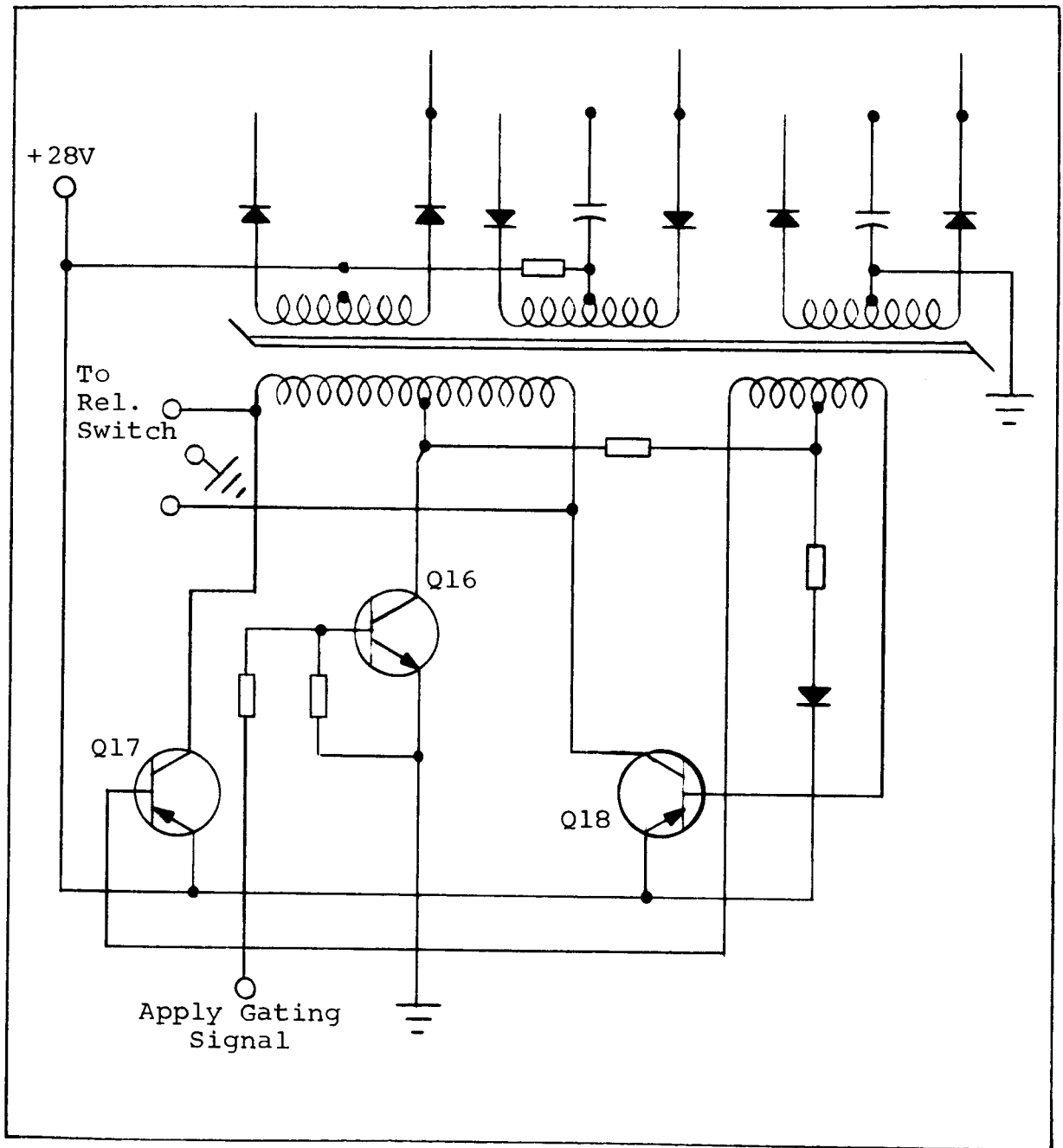


Figure 6. Oscillator and DC Drives

Since all drive voltages are supplied by the oscillator, no power will be drawn from the 28 volt supply during the standby condition.

The basic oscillator is a core-timed multi-vibrator designed so that the saturating element of the oscillator does not have to carry the reluctance switch primary current. The 10 kc/s output of the oscillator is fed directly to the reluctance switch with no attempt to modulate the pulse width at this point. Pulse width modulation at this point is unsatisfactory, since it interferes with the rate sensing information that is taken from the reluctance switch output windings.

b. Reversing Bridge

In the earlier effort on NASA contract NAS-5-3934, two magnetic rotor - position sensors were used to obtain forward and reverse rotation. The present circuit eliminates one of the position sensors and retains a bi-directional drive capability.

The direction of rotation is dependent upon the relative position of the position sensor rotor, with that of the motor rotor. Changing their relative positions by 180 electrical degrees will reverse the torque. A solution to this problem would be to mechanically shift the position of the position sensor rotor with respect to the motor rotor. Functionally, this is not a practical solution. Therefore, it must be accomplished statically in the electronic circuit. The connection diagrams for forward and reverse rotation are shown in Figures 7 and 8.

Observing these two figures, it is seen that reverse rotation is accomplished by reversing the input signals to the transistor switches in each leg of the three phase commutator bridge. This is further substantiated by constructing the armature switching sequences, Figure 9, the current flow diagrams, Figure 10, and finally looking at the vector diagrams in Figure 11. These vector diagrams show the resultant armature fields for two positions in the forward and reverse cycles. It should be noted that in position 1, for both the forward and reverse switching sequence, sensor windings 3 and 4 are excited. Comparing position 1 (forward) with position 1 (reverse) in Figure 11, it is shown that a 180 electrical degree shift in the armature field is obtained by reversing the input signals to the transistor switches in each leg of the three phase bridge. It is also shown in Figure 11 that the advancement from

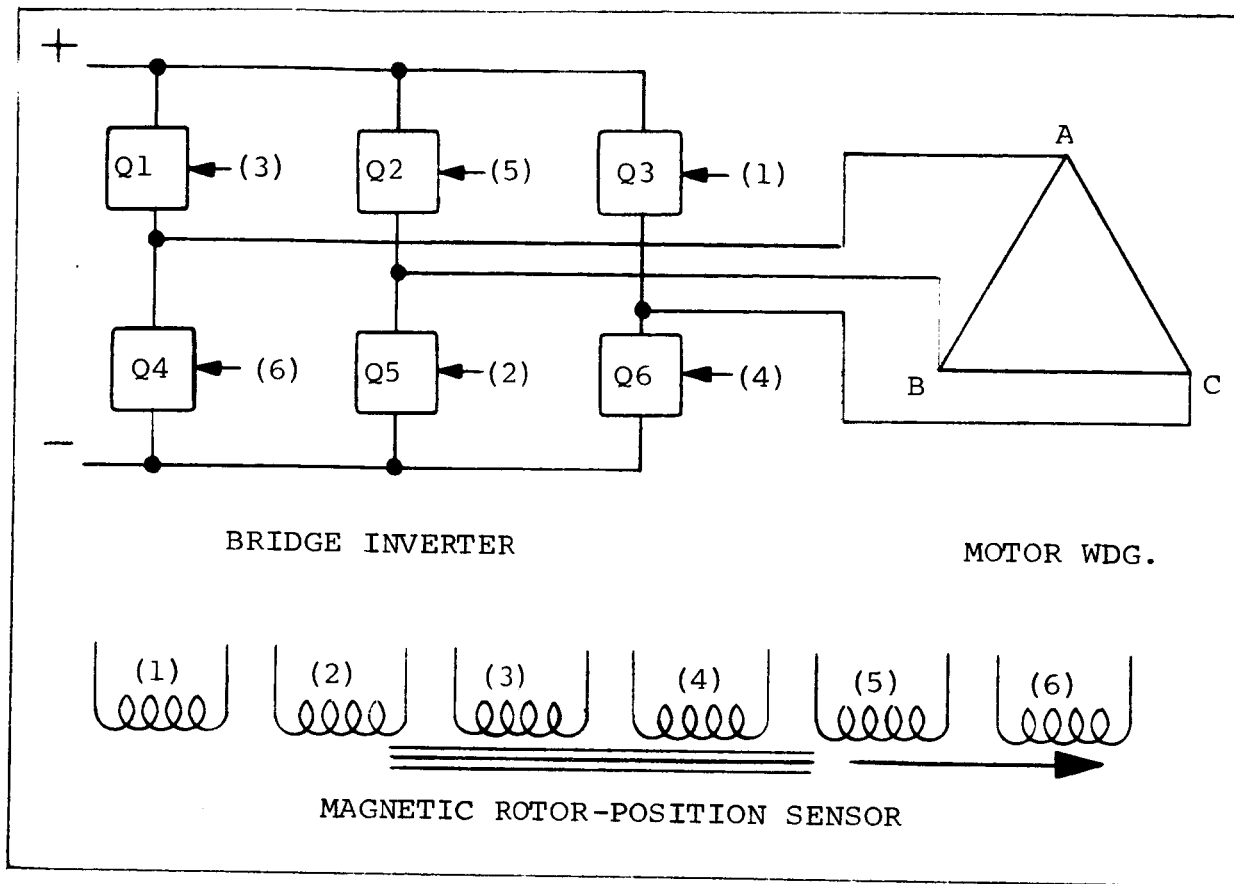


Figure 7. Connection Diagram Forward Rotation

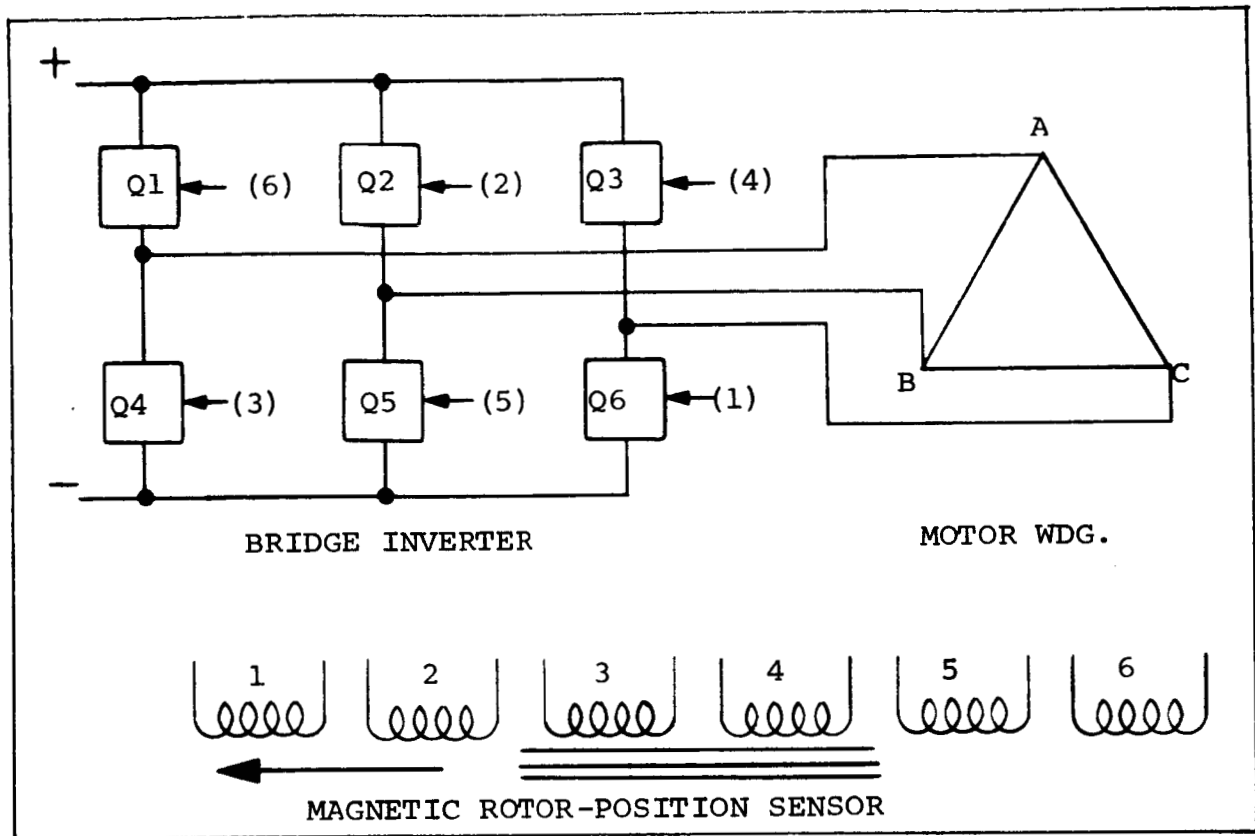


Figure 8. Connection Diagram Reverse Rotation

FORWARD ROTATION - REFER TO FIGURE 7

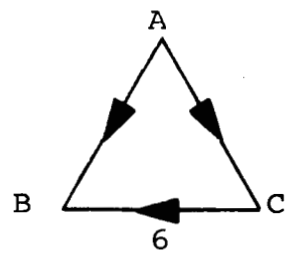
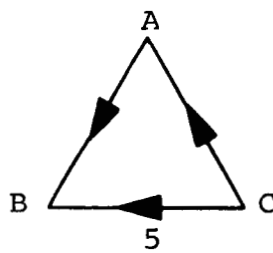
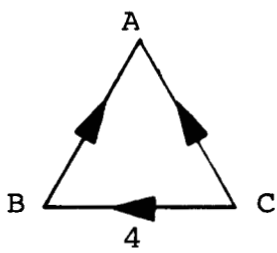
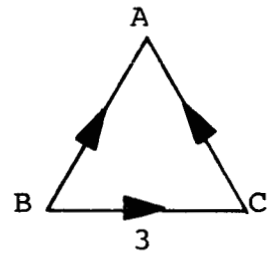
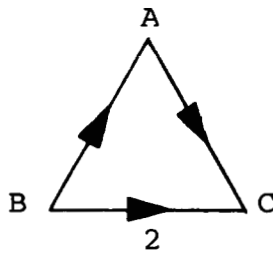
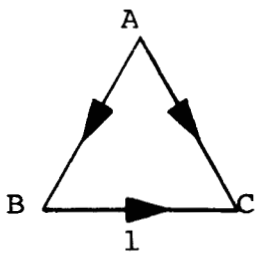
POSITION	SENSOR WINDINGS EXCITED	TRANSISTORS "ON"
1	3 - 4	Q1 - Q6
2	4 - 5	Q6 - Q2
3	5 - 6	Q2 - Q4
4	6 - 1	Q4 - Q3
5	1 - 2	Q3 - Q5
6	2 - 3	Q5 - Q1

REVERSE ROTATION - REFER TO FIGURE 8

POSITION	SENSOR WINDINGS EXCITED	TRANSISTORS "ON"
1	4 - 3	Q3 - Q4
2	3 - 2	Q4 - Q2
3	2 - 1	Q2 - Q6
4	1 - 6	Q6 - Q1
5	6 - 5	Q1 - Q5
6	5 - 4	Q5 - Q3

Figure 9. Armature Switching Sequence

FORWARD ROTATION



REVERSE ROTATION

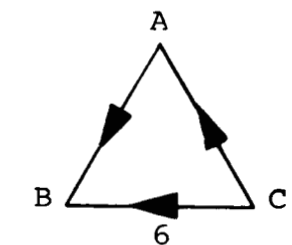
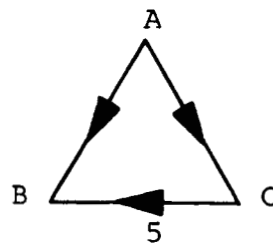
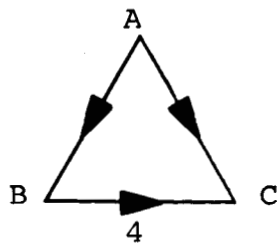
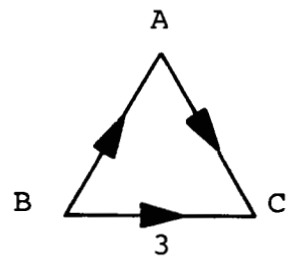
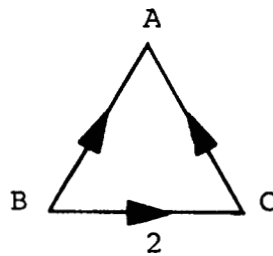
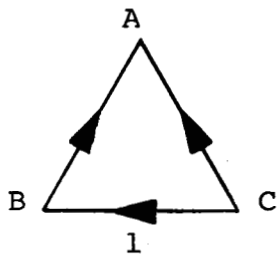


Figure 10. Current Flow Diagrams Delta Winding - Six Switching Positions

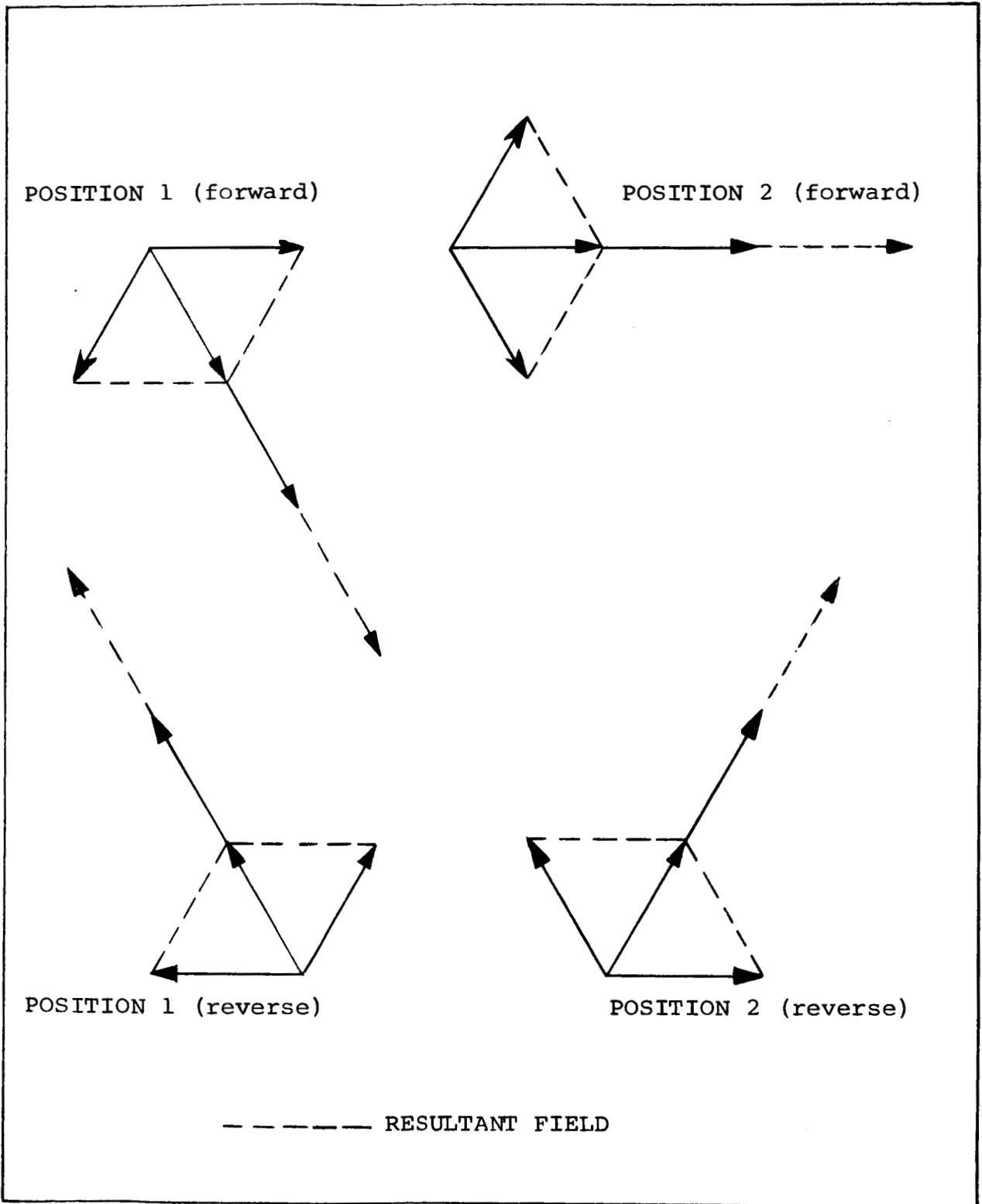


Figure 11. Vector Diagrams Showing the Resultant Fields for Two Positions in the Forward and Reverse Cycles

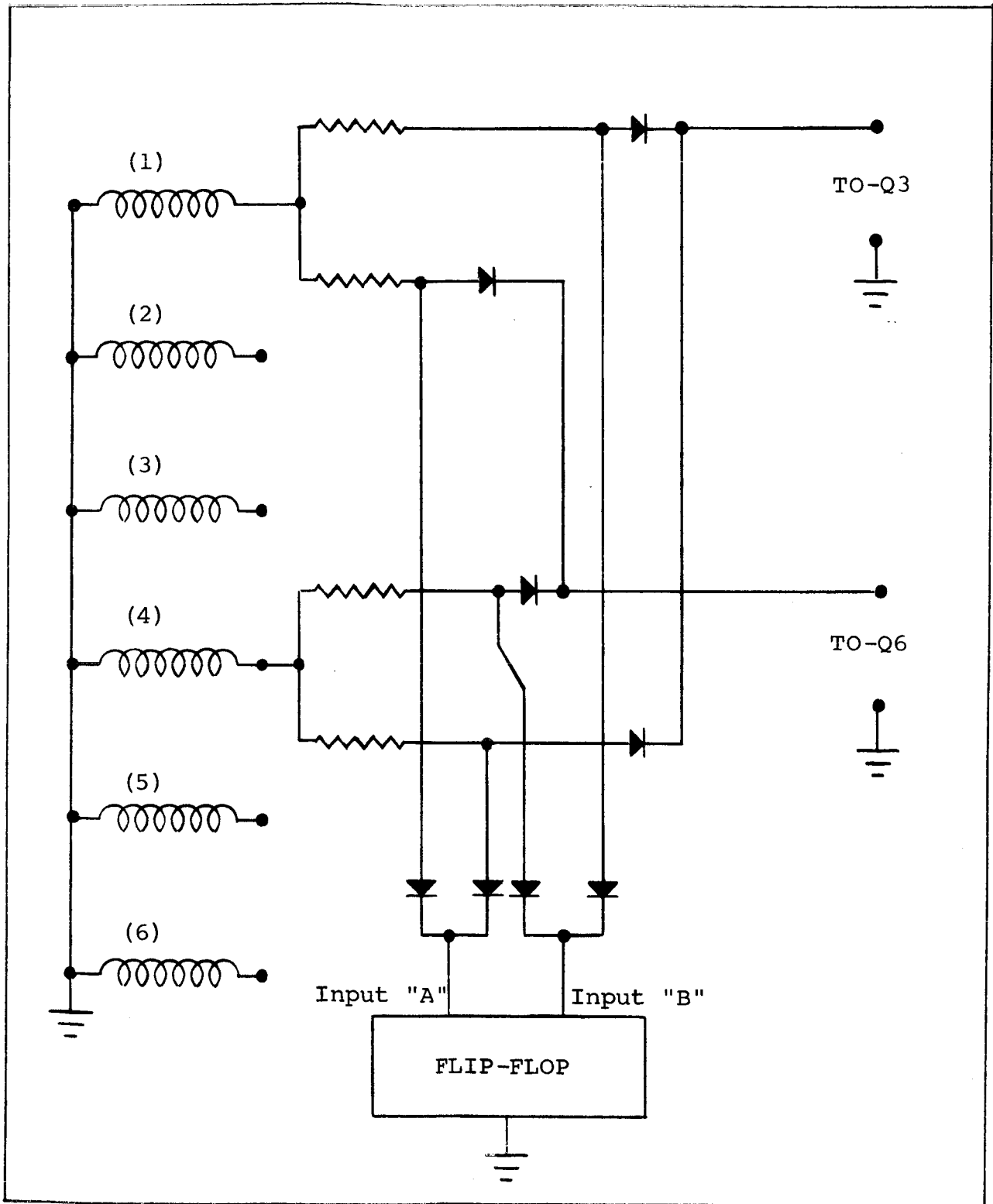


Figure 12. Diode Logic Reversing Circuit

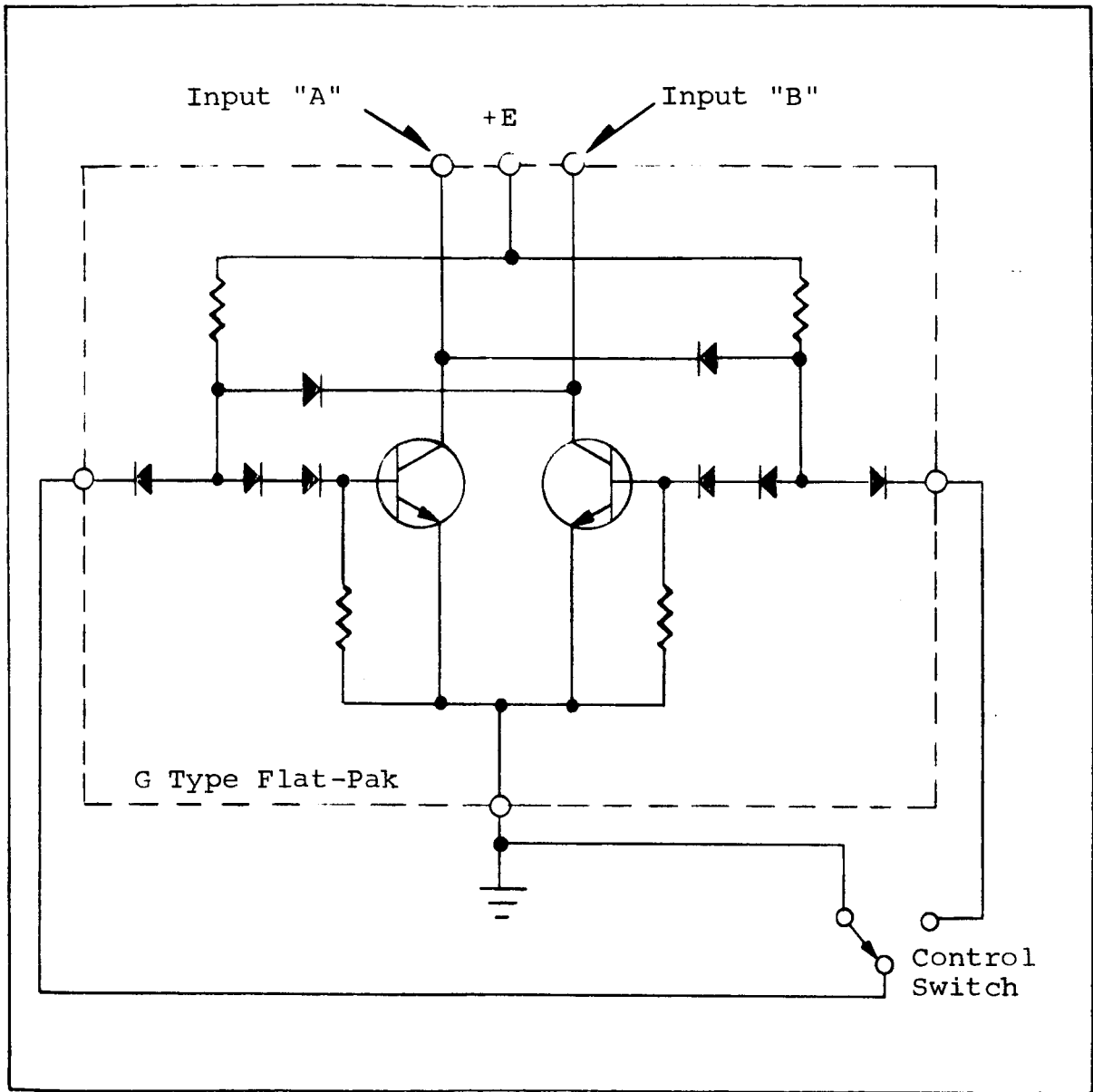


Figure 13. Diode Logic Circuit Flip Flop

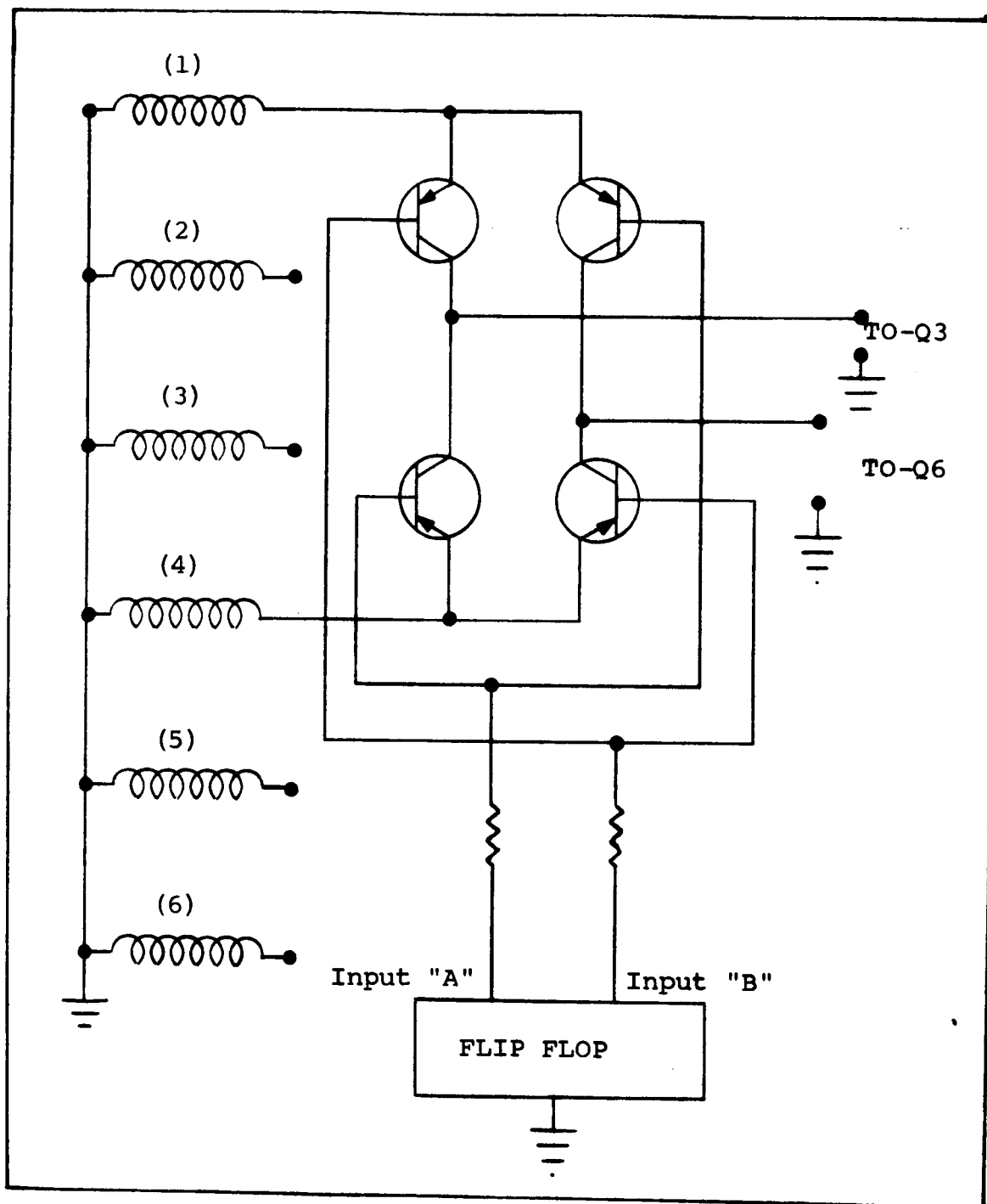


Figure 14. Transistor Reversing Bridge

position 1 (forward) to position 2 (forward) generates a field which rotates counterclockwise. The reverse cycle generates a field which rotates in a clockwise direction.

In this program, several methods of switching the input signals to the bridge transistors were considered. Among these were (1) using saturating transformers, (2) using diode logic as shown in Figure 12, and (3) using the transistor bridge shown in Figure 14. In each case, only one magnetic rotor-position sensor and one set of sensor windings are required. The saturating transformer method had some basic operational problems, besides being complex, and was given very little consideration. The basic theory was to change control by reversing the bias on a saturating transformer.

Figure 12, which shows the second method for obtaining bi-directional drive, uses diode logic to obtain reversal of the drive signals. Reversal is obtained by grounding either input "A" or input "B".

A flip-flop such as that shown in Figure 13 can be used to ground either input. It is desirable to use a flip-flop to perform this function because it provides a lock, that is, either input "A" or "B" will always be tied to ground, preventing an ungrounded condition. If both inputs are ungrounded, both transistors in the leg of the bridge will turn on, causing a short circuit. Figure 12 shows the bi-directional drive circuit for only two of the sensor windings. The circuit must be repeated for the other two sets of sensor windings; however, only one flip-flop is required for each system.

Figure 14 shows a third method of obtaining reversibility. This method utilizes a "transistor bridge" to give the correct logic. Reversal is obtained by grounding either input "A" or input "B". Grounding input "A" activates one pair of diagonal transistors, thus giving one direction of rotation. Grounding input "B" activates the other pair of diagonal transistors, thus giving the reverse direction of rotation. Reverse rotation is obtained by switching the signals from the two reluctance switch windings to the upper and lower bridge switches in each leg of the armature control bridge.

The transistor bridge reversing scheme was selected for the final circuit because of its simplicity and improved reliability. A total of 18 components, plus one flip-flop is required for this reversing scheme.

Should input "A" and input "B" both become ungrounded, no harmful effects will result. In this case, no signal from the reluctance switch will be conducted to the armature switches, and motor operation will cease.

The flip-flop shown in Figure 15 can be used with the transistor bridge reversing scheme since one of "A" and "B" need not be tied to ground at all times.

Addition of the two diodes provides a signal to activate the oscillator when either a forward or reverse gate signal is applied to the flip-flop. With neither a forward nor reverse gate signal applied, the entire circuit is in the standby condition.

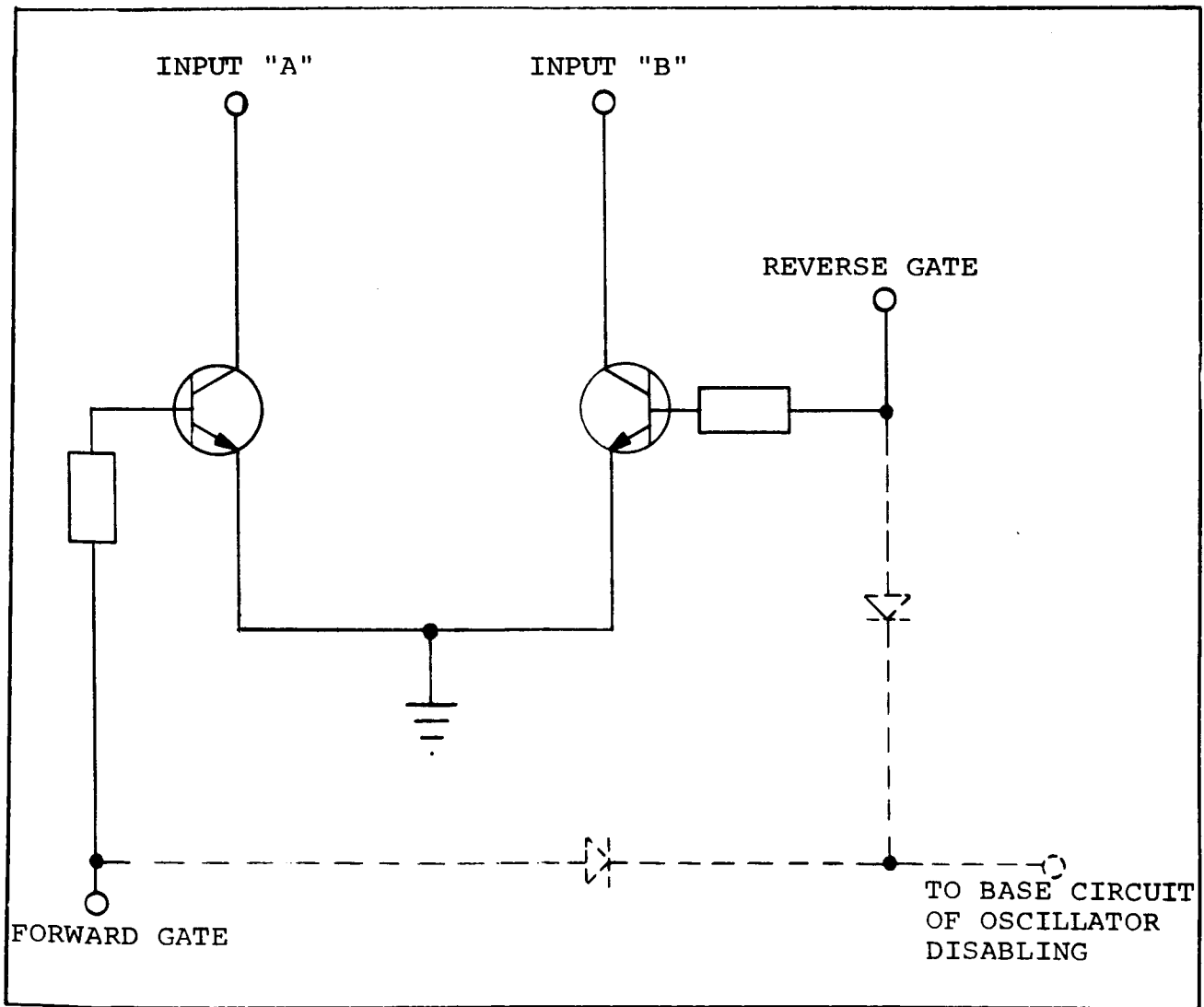


Figure 15. Transistor Reversing Bridge Flip-Flop

c. Regenerative Trigger

It has been established that the controller-commutator circuit must drive the armature switches regeneratively to permit operation at the stall condition for any angular position of the rotor without damage to the circuit.

The trigger used in the circuit is a basic level detecting regenerative Schmidt Trigger. The triggering level of the Schmidt Trigger is established by the value of the resistance in the emitter circuit. Increasing the value of this resistance also increases the trigger's hysteresis. An integrated circuit Schmidt Trigger will be used to save space and to increase reliability, speed, and efficiency. The Westinghouse type T package (similar to a TO-5 transistor can) has been selected because of its rigidity and mounting simplicity.

The basic Schmidt Trigger inherently has a certain amount of hysteresis which can be changed as mentioned above. It should be noted at this point that the lock-out scheme, to be discussed later, makes the controller commutator operation independent of the Schmidt Trigger's hysteresis.

d. Commutator Bridge

In order to maintain conservative design margins, it is necessary to drive the armature switches with enough current to completely saturate them at locked rotor collector currents. This requires that the base drive current for the armature switches be relatively high with actual value depending on the gain of the transistor used. To keep drive losses down, it is necessary to supply the drive current with as small a voltage as practical. The most efficient method to obtain the drive current is with an isolated power supply of 4 to 6 volts which can be obtained from the oscillator with the addition of a winding and two rectifiers.

The base-emitter circuits of the top row switches have both a drive voltage and a reverse bias voltage supplied by the oscillator. The reverse bias voltage is supplied continually through R7, R11 and R15. The base drive current is supplied at a 10 kc/s rate to the appropriate armature switch by the isolated drive winding through R16 and either Q7, Q9 or Q11, depending on which Schmidt Trigger is activated.

The bottom row switches have a base drive voltage applied from the third supply of the oscillator. This is the same supply that provides voltage for the Schmidt Triggers. The base drive current is directed to the appropriate armature switch through Q13, Q14 or Q15, depending on which bottom Schmidt Trigger is active. The base drive current for the bottom row switches is not switched on and off at a 10 kc/s rate like the top row switches (the reason will be discussed later). During the time that the driver transistor is saturated, the armature switch drive current is conducted through the saturated driver.

The capacitor C3, C4 or C5, associated with that driver, discharges through the driver's collector-emitter circuit. During the half cycle that the Schmidt Trigger is not active, the driver transistor is cut-off and the capacitor's charging current supplies enough base drive to keep the armature switch saturated until the next half cycle.

The lower armature switches are driven at a 100% duty cycle.

e. Lockout Circuit

To minimize ripple torque and eliminate dead spots, two conditions must be met (1) at any one time, two and only two armature switches must be on and (2) transfers from one armature switch to the next switch must take place without appreciably changing the torque level at that shaft position. These conditions must be met within the supply voltage range of 22-34 volts, and in either direction of motor rotation.

Refer to Figure 16. The crossover point is defined as the shaft position at which the output voltage at one reluctance switch secondary winding equals the output voltage of the next secondary winding. The crossover position is independent of applied voltage and the direction of rotation. The circuit has been designed to take advantage of this unique situation by transferring from one switch to the next switch at the crossover point in both the top and bottom row switches.

Diodes CR1, CR2, CR3, CR4, CR5, and CR6 provide the proper logic for the lockout scheme. Refer to the top three Schmidt Triggers of Figure 5. When the first Schmidt Trigger is activated, the input signals to the other two Schmidt Triggers are grounded through transistor Q8 and diodes CR2 and CR4. Initially the Schmidt

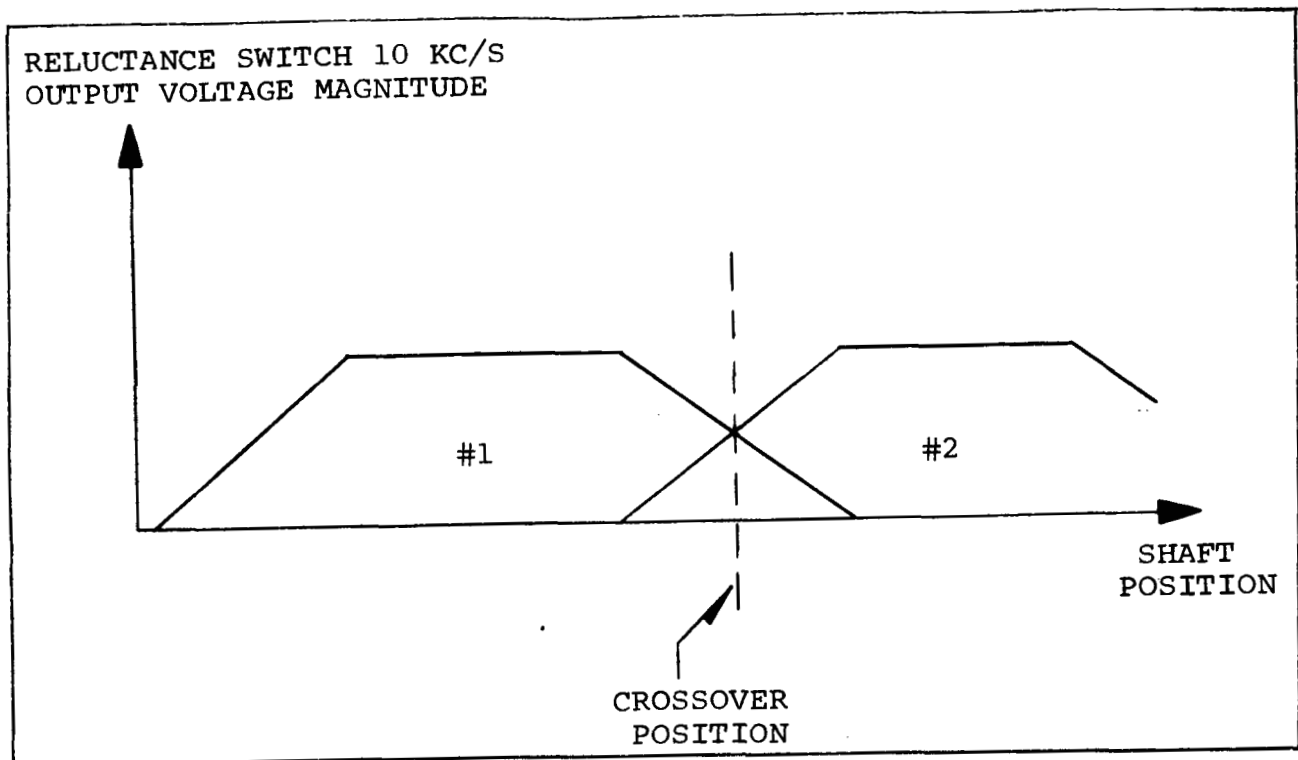


Figure 16. Crossover Point Position

Trigger that has the highest magnitude input signal from the reluctance switch is the trigger that will be activated first, thus locking "off" the remaining two triggers. This logic takes place at the beginning of each positive 10 kc/s pulse received from the reluctance switch output. As a result, the Schmidt Triggers are functioning as level comparator switches rather than level detecting switches. Since the interlock logic takes place on a 10 kc/s basis, transfer occurs exactly at the crossover point.

The same situation applies to the bottom row switches.

f. Pulse-Width Modulator

The permanent magnet rotor generates a back emf in the stator winding as the rotor turns. The speed at which the motor runs is then determined by the applied voltage and shaft load. The speed tends to increase in order to balance the generated back emf and the applied voltage.

Since the armature switches are turning on and off at a 10 kc/s rate, and since the time constant of the armature winding is very long compared to this rate, speed control can be obtained by varying the on to off time ratio of the armature switches (pulse-width modulation).

The inductance of the armature winding is such that the reactance at 10 kc/s is very large compared to the resistance. As a result the 10 kc/s current, being limited by the winding reactance, will be small but the d-c current, being limited by the winding resistance, will be large.

The maximum duty cycle of the 10 kc/s armature switches is: on for 50 u-sec and off for 50 u-sec. That is, a 50% duty cycle. The resulting d-c current flow will be one half of the applied 28 volts, divided by the winding resistance. Neglecting losses, the no-load speed of the motor will be just great enough to generate a back emf of 14 volts. Reducing the duty cycle below the maximum 50% value reduces the effective level of the applied motor voltage proportionally, and the motor speed reduces accordingly. The duty cycle can be reduced to zero, giving no torque or motor rotation.

It has been established that switching both the top and bottom armature switches at a 10 kc/s rate will not give rise to significant net d-c armature currents.

Figure 17a depicts an equivalent circuit of the case where a 50% duty cycle is used in both top and bottom armature switches.

During the period of time that the top and bottom transistors are saturated, a current begins to flow and builds up flux in the armature core. Both transistors cut off after 50 u-sec and the armature windings commutate through the commutating diodes and the 28-volt supply. Current begins to decay as the diodes clamp the armature commutating voltage to -28 volts. This results in a 10 kc/s a-c voltage being applied to the armature winding with negligible value of d-c voltage. The current, being limited by the high reactance is very small and does not contribute significantly to torque.

To overcome this problem, either the top row or the bottom row of armature switches must have a 100% duty cycle, while the remaining row of armature row of armature switches has the pulse width modulated 50% duty cycle.

Figure 17b will verify the point. When the top transistor is saturated, the current starts to build up. When cutoff is reached, the winding commutates through one diode and the bottom transistor which is still

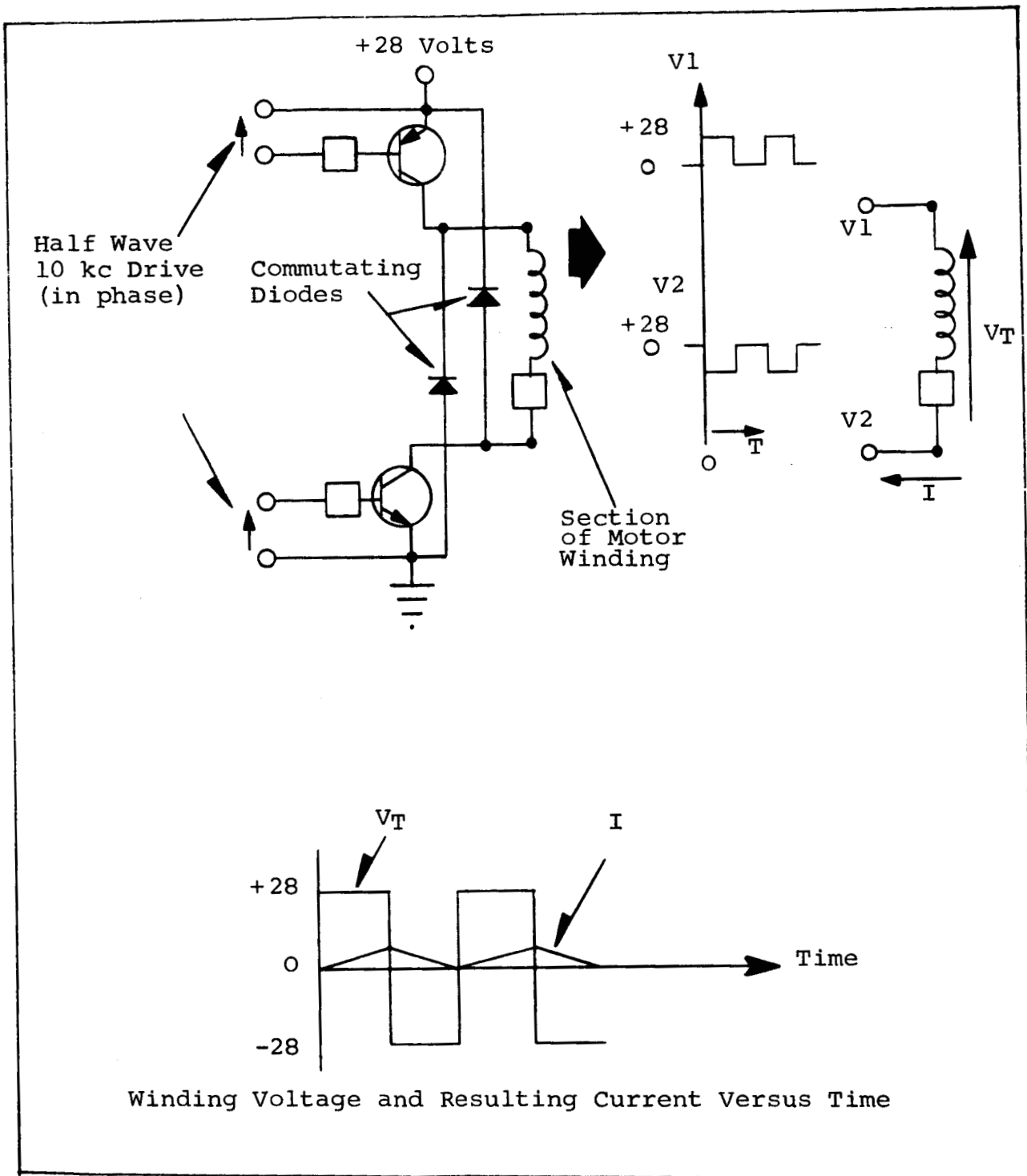


Figure 17a. Equivalent Circuit of Armature Winding with Top and Bottom Switches Operating at 10 kc/s

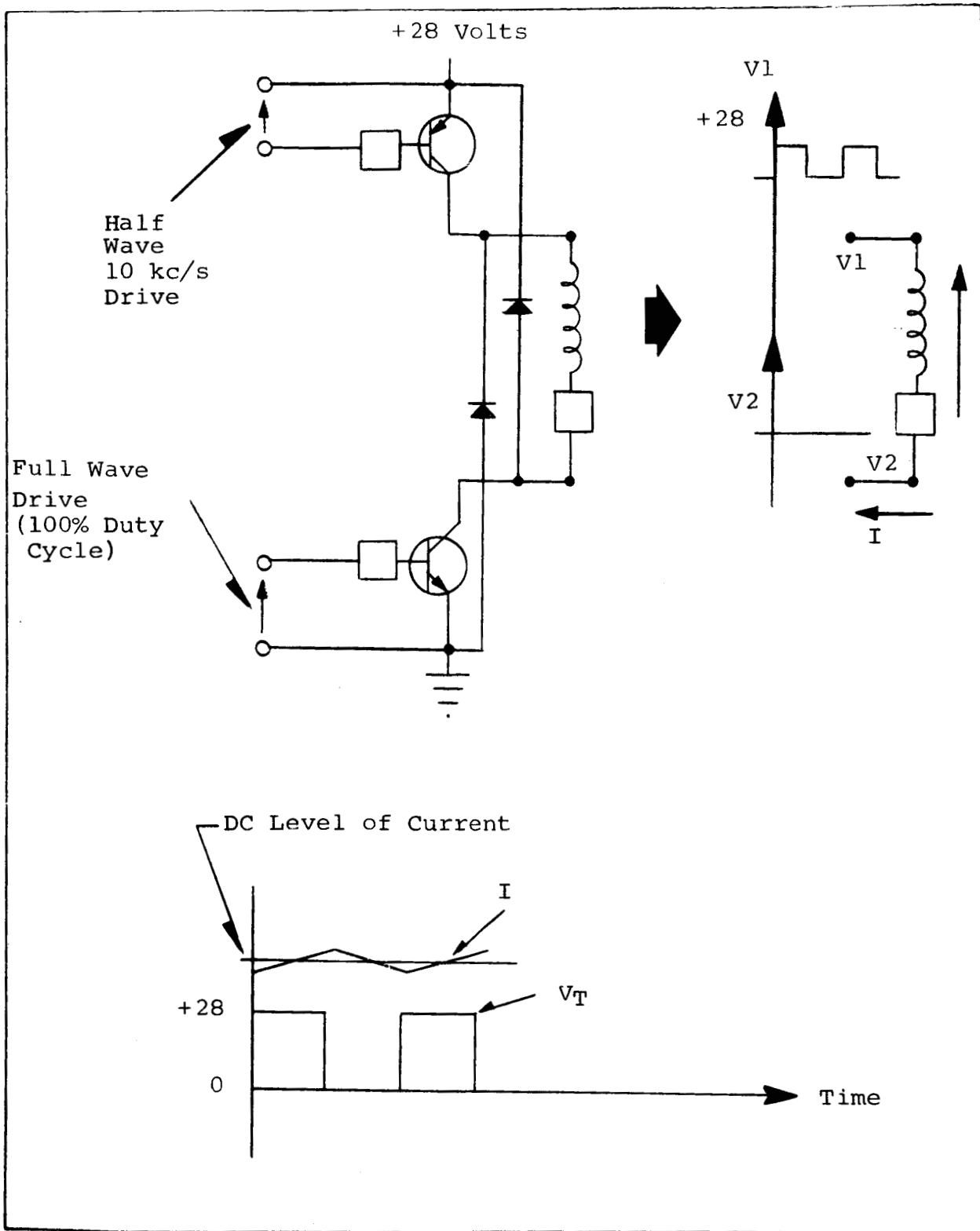


Figure 17b. Equivalent Circuit of Armature Winding with Top Switch Driven Half Wave and Bottom Switch Driven Full Wave

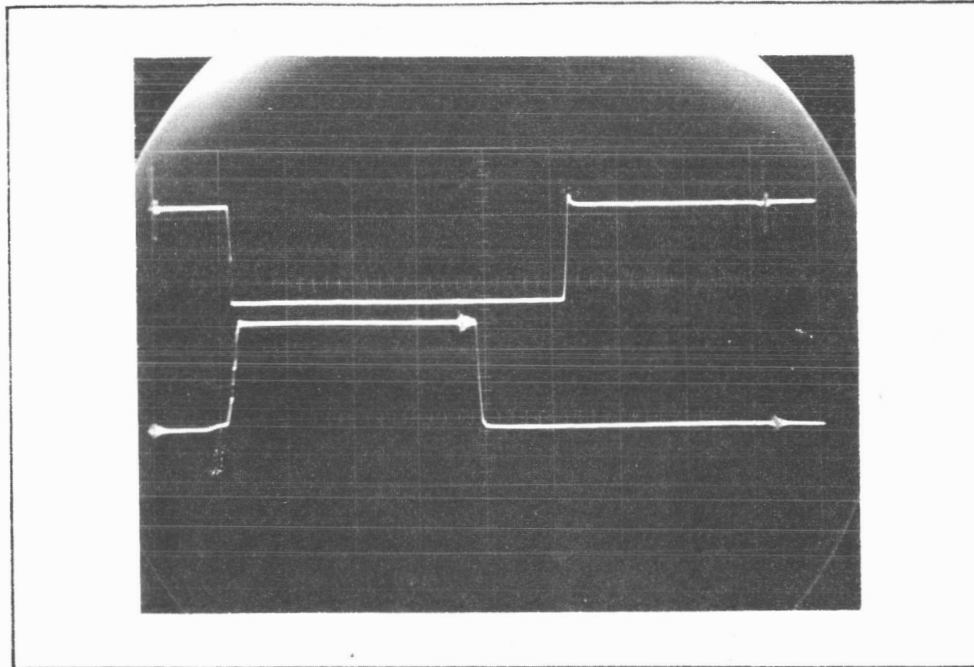
conducting because of the 100% duty cycle. The commutating voltage is now clamped to zero volts rather than -28 volts. As a result, the armature winding voltage never goes negative and has an effective value of d-c voltage applied. This gives rise to a d-c current with only a very small 10 kc/s ripple component. The d-c current level, limited by the winding resistance, results in a net motor shaft torque. Hence, the effective applied armature voltage and the resulting current flow is directly proportional to the duty cycle of the top armature switches.

To be conservative, the armature switches must be driven with enough current to insure saturation at locked rotor collector currents. This relatively high drive current causes the armature switch storage time to increase a significant amount. The storage time of a hard driven transistor is shown in Figure 18a. It can be noted that the transistor continues to conduct, even though its base drive has been removed. As a result, the effective applied armature voltage will not vary directly with the base drive duty cycle. Also the storage time of the transistor is subject to change with temperature. The resulting open loop speed control of the motor would be unreliable. Hence, the storage time of the transistor must be effectively eliminated to obtain linear open-loop speed control. The method used to eliminate the transistor storage time is to back bias the base-emitter junction of each of the armature switches during the period when forward base drive is zero. The result of the reverse bias addition is shown in Figure 18b. The storage time is small enough to be neglected.

The armature switches are pulse-width-modulated by a saturable reactor placed in series with a current limiting resistor in the base drive circuit of only the top row switches.

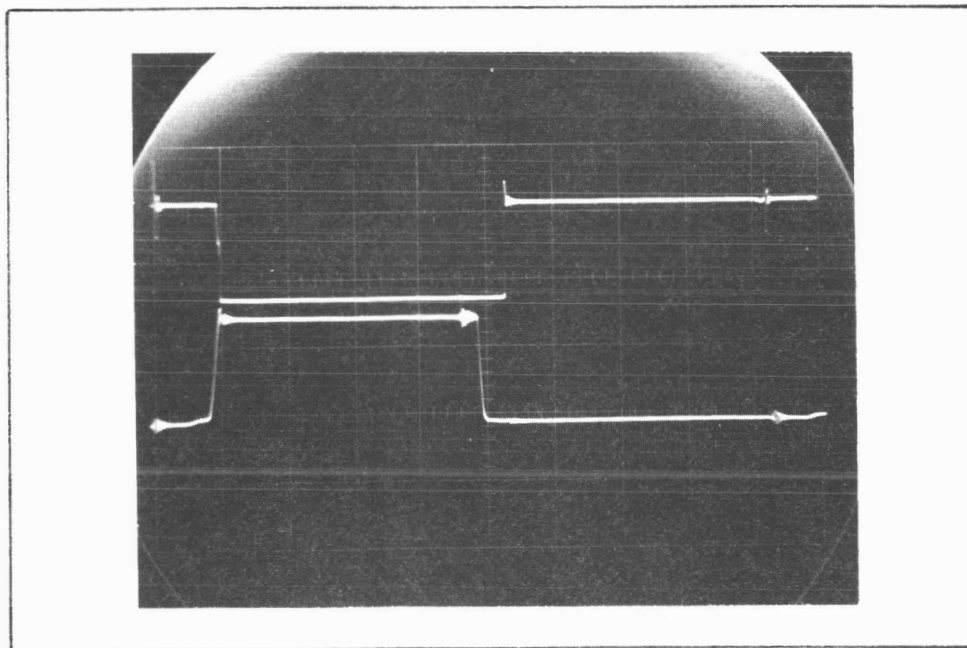
Since only one of the three switches is on at any one time, only one saturable reactor is required in the common return path. A permanent reset bias is applied to the saturable reactor through resistor R_1 , and the bias winding. The control winding has a variable 0-15 volt external supply for speed control.

The entire base-emitter drive circuit for the top row pulse-width-modulated armature switches, consists of the driver switches, Q7, Q9, and Q11, the saturable reactor, the current limiting resistor R_{16} , and the isolated 4 volt drive from the oscillator.



TOP: Collector to emitter voltage of armature switch and
 BOTTOM: Base drive to armature switch without back bias vs.
 time = 10 u-sec per cm

Figure 18a. Armature Switch Storage Time Without Bias



TOP: Collector to emitter voltage of armature switch and
 BOTTOM: Base drive to armature switch with back bias vs.
 time = 10 u-sec per cm

Figure 18b. Armature Switch Storage Time With Bias

With the external 0-15 volt supply set at zero volts, the saturable reactor has full reset applied by the bias winding. This allows the reactor to drop the entire 4 volt drive voltage across the gate winding for the half cycle that the driver switch is saturated. During the remaining half cycle, the driver switch is cut off and the core is reset by the permanent bias winding, resulting in no motor rotation.

Increasing the external control to 15 volts saturates the reactor completely. None of the drive voltage is supported across the reactor's gate winding. This results in full current drive to the armature switches during the half cycle that the driver switch is saturated, giving 50% duty cycle and full motor speed.

The amount of external control applied between zero and 15 volts determines the amount of reset applied to the reactor and hence the length of time the gate winding will drop the 4 volt base drive voltage. Since the saturable reactor operates on a volt-second basis, the time required before the drive voltage saturates the core is directly related to the amount of reset which is in turn inversely related to the external control. Hence the drive current pulse width or the duty cycle is directly proportional to the applied external control and the motor speed is directly proportional to the external bias voltage in the zero to 15 volt range. Figure 19 illustrates the theoretical speed versus control (external bias) voltage characteristic curve of the circuit. Experimental data indicated that the theoretical curve was approached. Some minimum voltage is required for the motor to overcome its own static friction so that the zero speed point did not exactly occur at zero bias and would tend to vary because of variation in friction and cogging torque. Also it would be difficult to obtain full speed at exactly 15 volts. However, the operation was stable at the two end points.

Increasing the control voltage above 15 volts only drives the reactor further into saturation, but since it saturates at 15 volts, the speed cannot increase further because the duty cycle is limited to 50% by the driver transistors. A negative external control tends to reset the core faster. As a result, the drive current remains zero because the reactor still drops the 4 volt drive voltage and the motor does not run.

2. Reliability

The entire controller commutator circuit has a total of 152

the top switches. This loss varies from zero to approximately 0.9 watts maximum.

Table 2 gives a breakdown of the estimated watts lost in the controller commutator. These values are based on a full speed motor setting (a 50% duty cycle on the upper armature switches).

TABLE 2
LOSSES IN CONTROLLER COMMUTATOR

	<u>Watts</u>
Oscillator Drive and Losses	0.10
Reluctance Switch Losses (estimated max.)	0.40
Reversing Bridge Drive and Voltage Divider	0.02
Schmidt Trigger Drive	0.06
Bottom Row Armature Switch Drive	0.50
Bottom Row Armature Switch Driver Drive	0.01
*Top Row Armature Switch Drive	0.25
*Top Row Armature Switch Driver Drive	0.02
*Top Row Armature Switch Reverse Bias	0.05
Pulse Width Modulator Permanent Bias	0.01
Other	0.40
TOTAL	1.82
*Will decrease as duty cycle is decreased below 50%	

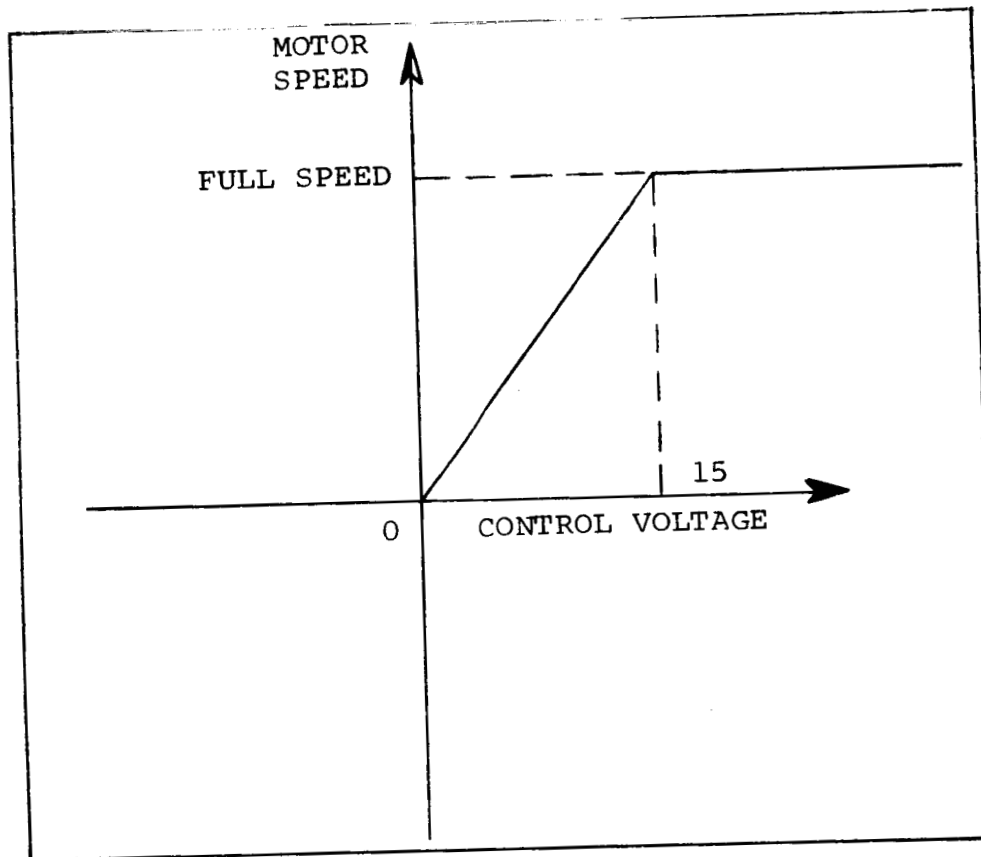


Figure 19. Speed Control Characteristics

discrete components. The use of integrated circuit Schmidt Triggers reduces the complexity and physical size, and increases the reliability by reducing the number of solder connections and other factors. By counting an integrated Schmidt Trigger as one component, the number of components drops to 116.

The area of integrated circuits will be investigated further in an effort to reduce the number of components below 116 and increase the reliability. It is believed that the diode lockout circuits and possibly the transistor reversing bridges can be obtained in the form of integrated circuitry.

3. Efficiency

For a given motor speed torque setting, the losses within the controller commutator are fixed except for the power dissipated in the armature transistors. That is, as the motor load increases, the resulting increase in motor current causes an increase in commutating losses only at the armature switches. That power is the collector to emitter saturation voltage, times the motor current, for the bottom switches and also, times the fraction of duty cycle, for